**Title**
STUDY OF SELF-FOCUSING AND SMALL-SCALE FILAMENTS OF LIGHT IN NONLINEAR MEDIA



**Author**
Loy, M.M.T.

**Publication Date**
1971-12-01

STUDY OF SELF-FOCUSING AND SMALL-SCALE FILAMENTS OF LIGHT IN NONLINEAR MEDIA.

Loy, M. M. T.; Shen, Y.R.

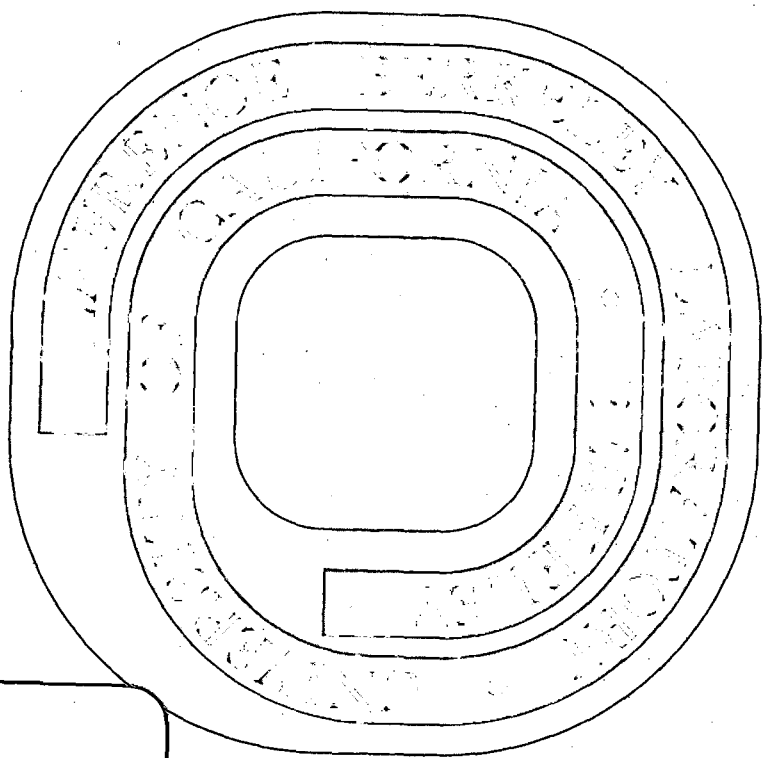

## DISCLAIMER

Submitted to The Physical Review

LBL-431
Preprint



UNIVERSITY OF CALIFORNIA

Lawrence Berkeley Laboratory
Berkeley, California

AEC Contract No. W-7405-eng-48

# STUDY OF SELF-FOCUSING AND SMALL-SCALE FILAMENTS OF LIGHT IN NONLINEAR MEDIA

M. M. T. Loy† and Y. R. Shen

December 1971

LBL-431

# Study of Self-Focusing and Small-Scale Filaments of Light in Nonlinear Media

M. M. T. Loy† and Y. R. Shen

Department of Physics, University of California
and
Inorganic Materials Research Division,
Lawrence Berkeley Laboratory,
Berkeley, California 94720

## ABSTRACT

It is shown that the small-scale filaments generated by laser pulses in nonlinear media are the natural consequence of moving foci. Many controlled experiments performed with single-mode Q-switched laser pulses are described. The results are difficult to be explained by the self-trapping model, but agree very well with the predictions of the moving focus model. The earlier experimental results on filaments reported in the literature are shown to be consistent with the moving focus model. It is seen that the appropriately modified moving focus model can also explain qualitatively the observed filament characteristics in the picosecond case. Many unsolved theoretical and experimental problems on self-focusing and small-scale filaments are discussed.

## I. INTRODUCTION

It is well-known that the refractive index of a medium is a function of the beam intensity. In most media, the refractive index increases with the beam intensity. When an intense laser beam with a bell-shape spatial intensity profile propagates in such a medium, the central part of the beam sees a larger refractive index than the edge, and therefore, travels with a slower velocity. Accordingly, the wavefront gets distorted, and since light should propagate along the normals to the wavefront, this leads to focusing of the beam. This induced lens effect is known as self-focusing. However, a beam with a finite cross-section would normally diffract. It will self-focus only if the self-focusing strength due to the induced refractive index overcomes the diffracting strength. In an ideal case, when the self-focusing strength just balances out the diffracting strength, the beam should propagate in the medium with its cross-section remained unchanged. This is known as self-trapping.

Askarjan,[1] Talanov,[2] and Chiao, Garmire, and Townes,[3] were the first ones to point out the possibility of self-trapping of light in a nonlinear medium. Subsequently, Kelley,[4] Talanov,[5] and Akhmanov et al.[6] investigated theoretically the dynamics of self-focusing. Results of early experiments[7-11] basically agreed with their predictions for self-focusing.

However, it was first observed by Chiao et al.[12] that a self-focused beam appears to break into intense streaks after self-focusing. These streaks are typically several microns in diameter,[12,13] and can last over a distance of a few cm.[7,14,15] They were called small-scale filaments by Chiao et al.[12] It was suggested that self-trapping should be responsible for these streaks, but theoretical attempts using the

self-trapping model to explain the observations were not successful.[16-20] In particular, it was not clear how a self-focused beam can turn into a self-trapped filament (or filaments).[17-19]

A different model was then proposed by Lugovoi and co-workers[21] to explain the observed streaks. They noticed that pulsed lasers were used in these experiments. As seen from the self-focusing description, the focal spot resulting from self-focusing of the beam should move along the axis with time in accordance with the time variation of the laser power during a pulse.[22] The streaks observed on time-integrated photographs should then correspond to the tracks of the moving focal spots, with their diameters equal to the diameters of the focal spots. With a single-mode laser beam, only a single streak is expected, but with a multi-mode laser beam, many streaks can be the result.

Experimentally, results obtained under different conditions by different groups are usually very different. Consequently, interpretations of the results have also been very different. For example, results obtained with multi-mode Q-switched lasers[12-15,23] or mode-locked lasers[24-27] were often used to support the self-trapping model. On the other hand, our results,[28-30] and those of others[31-34] obtained with single-mode lasers showed definitely that the streaks were formed by moving foci. It is apparent that the streak (or filament) characteristics must depend critically on the input conditions, but a correct model should be able to explain all the observations, at least qualitatively. In this respect, the moving focus model, properly extended, appears to be rather successful. The purpose of this paper is three-fold: first, to give a more complete account of our experiments on self-focusing and small-scale filaments; second, to show that both our

results and those of others can be explained by the moving focus model; and third, to provide an up-to-date assessment on the problem in general.

In Section II, we give a brief review on the theories of self-focusing and small-scale filaments. Then, in Section III, we describe our experimental investigation on the problem under controlled input conditions, and show that our results and those of others with nanosecond laser pulses can be understood with the moving focus model. In Section IV, we discuss the many unsolved problems on self-focusing and small-scale filaments with nanosecond input pulses. Finally, in Section V, we show how the moving focus model, properly modified can also explain qualitatively the experimental results obtained under picosecond pulse excitation.

## II. REVIEW OF THEORETICAL CALCULATIONS

### A. Calculations on Self-Focusing

Let us consider a medium whose refractive index can be written as

$$n(|E|^2) = n_o + \Delta n\ (|E|^2) \tag{1}$$

where $\Delta n$ is the field-induced refractive index. In the steady state, if the field intensity is not too strong, we can expand $\Delta n = \Delta n_o$ into a power series of $|E|^2$.

$$\Delta n = \Delta n_o = n_2|E|^2 + n_4|E|^4 + \ldots . \tag{2}$$

The physical mechanisms for $\Delta n$ can be liberation of molecules, molecular reorientation and redistribution, electrostriction, and deformation of electronic clouds,[3] but for liquids with large Kerr constants under nanosecond or picosecond excitation, the effect of molecular reorientation usually dominates.[35] In this paper, unless specified, we shall be dealing with Kerr liquids. We shall assume for Kerr liquids that $\Delta n$ obeys the following relaxation equation.[36]

$$[(\partial/\partial t) + (1/\tau)]\Delta n = \Delta n_o/\tau \tag{3}$$

where $\tau$ is the relaxation time for molecular orientation and is of the order of a few picoseconds.

We now consider wave propagation in such a medium. The wave equation is given by

$$\nabla^2 E - (\partial^2/c^2\partial t^2)\,[(n_o + \Delta n)^2 E] = 0. \tag{4}$$

We can write $E = (1/2)\,\mathcal{E}(r,z,t)\exp(ikz - i\omega t)$, where $\mathcal{E}(r,z,t)$ is a complex function and $k = \omega n_o/c$. Then, with the higher-order terms neglected, Eq. (4) reduces to the form[6,17,37]

$$\left[\frac{\partial^2}{\partial r^2} + \frac{1}{r}\frac{\partial}{\partial r} + 2ik\frac{\partial}{\partial z} + 2i\omega\frac{\partial}{\partial t} + \frac{\Delta n}{n_o}k^2\right]\mathcal{E} = 0. \tag{5}$$

If we transform the coordinates $(r,z,t)$ to the moving coordinates $(r,\ z,\ \xi = t - zn_o/c)$, then the equation becomes

$$[\frac{\partial^2}{\partial r^2} + \frac{1}{r}\frac{\partial}{\partial r} + 2ik\frac{\partial}{\partial z} + \frac{\Delta n}{n_o}k^2]\mathcal{E}(r,z,\xi) = 0. \quad (6)$$

Correspondingly, Eq. (3) becomes

$$[(\partial/\partial\xi) + (1/\tau)]\Delta n = \Delta n_o/\tau. \quad (7)$$

By writing $\mathcal{E} = A(r,z,\xi)\exp[iks(r,z,\xi)]$, we can also separate Eq. (6) into two coupled equations for the amplitude A and the phase function s.

$$\frac{\partial A}{\partial z} + (\frac{\partial s}{\partial r})(\frac{\partial A}{\partial r}) + \frac{A}{2}(\frac{\partial^2 s}{\partial r^2} + \frac{1}{r}\frac{\partial s}{\partial r}) = 0 \quad (8)$$

$$2(\frac{\partial s}{\partial z}) + (\frac{\partial s}{\partial r})^2 = 2\frac{\Delta n}{n_o} + \frac{1}{k^2 A}(\frac{\partial^2 A}{\partial r^2} + \frac{1}{r}\frac{\partial A}{\partial r}). \quad (9)$$

In the steady-state case with a monochromatic wave, we have $\Delta n = \Delta n_o$. Equation (6) or Eqs. (8) and (9) can be solved analytically by the so-called paraxial-ray approximation,[6,17,37] but the quantitatively more correct solution has been obtained numerically. Kelley[4] did the first computer calculation. Subsequently, Goldberg et al.[18] and Dawes and Marburger[19] found the numerical solutions for a wide range of input laser power P. They showed that with $\Delta n_o = n_2|E|^2$ and for an input Gaussian beam with $P \gtrsim 1.5\,P_{cr}$, the beam tends to self-focus to a point at a distance

$$z_f = K/(\sqrt{P} - 0.858\sqrt{P_{cr}}) \quad (10)$$

where $K = (n_o a^2/4)(c/n_2)^{1/2}$, a is the variance of the Gaussian distribution.

and $P_{cr} = (1.22\pi n_o/k)^2(c/8n_2)$ is the critical power at which the beam would propagate in a self-trapped mode.[3] As a result of self-focusing, the on-axis field intensity increases as

$$I(z)/I(o) = [1 - (z/z_f)^2]^{-\alpha/2} \qquad (11)$$

with $\alpha$ close to unity. The rapid increase of I as $z \to z_f$ indicates that the focusing is extremely sharp. For this reason, the prediction of $z_f$ from the calculation should be reasonably good even though the assumption $\Delta n_o = n_2|E|^2$ may not be valid in the focus where the field intensity is high. Dawes and Marburger[19] also found that if the profile of the beam is non-Gaussian with a single maximum, then Eqs. (10) and (11) still hold with K replaced by Kf, where f is a dimensionless parameter of the order of unity, as suggested by Wang.[10] The critical power for self-trapping also increases as f increases.

Dyshko et al.[21] also solved Eq. (6) with a Gaussian input beam using a different numerical computing scheme. They found that for $P > 2P_{cr}$, there exist along the axis more than one focal spot. The number of which increases as P increases. However, for $P_{cr} < P < 2P_{cr}$, only one focal spot should appear at a position which seems to agree fairly well with $z_f$ of Eq. (10). In our later discussion, we shall assume $P < 2P_{cr}$, and that the position of the focal spot can be approximated by

$$z_f = K/(\sqrt{P} - \sqrt{P_o}) \qquad (12)$$

where K and Po are parameters determined directly from experiments.[10]

If the input laser beam is in the form of a pulse and if the pulse envelope does not vary appreciably within a relaxation time $\tau$ for molecular reorientation, then we have from Eq. (7), $\Delta n = \Delta n_o(|E(\xi)|^2)$. Consequently, the solution in the form of Eqs. (10) - (12) still holds, but P is now a function of $\xi$, and $I(z)/I(o)$ is replaced by $I(z,t)/I(o,\xi)$. If the pulse envelope varies appreciably in $\tau$, then we must find the self-focusing solution by solving Eqs. (6) and (7) simultaneously. Fleck and Kelley[38] did numerical calculation for $P_{max} = 12.5$ Pcr and for various pulsewidths $\delta t$ of the order of $\tau$, assuming $\Delta n_o = n_2|E|^2$. They found that the self-focusing distance $z_f$ increases with decreasing $\delta t$ as one would expect. For $\delta t/\tau = 0.475$, the self-focusing distance is about 4 times that of $\Delta t/\tau >> 1$.

B. Theoretical Models for Small-Scale Filaments

According to the early experimental observations,[12,13,15] a small-scale filament was a streak of intense light with a characteristic constant diameter, lasting for a length of a few cm and for a duration of the order of $10^{-10}$ sec. The induced refractive index $\Delta n$ in the filament appears to be around $10^{-3}$.[15]

It was then believed that these filaments were the result of self-trapping of light predicted earlier.[3] This self-trapping model could explain, only with the help of further assumptions, most of the observations qualitatively.[15] For example, the finite length and duration of a filament could be understood if we assume heating of the medium through stimulated Raman scattering would destruct and terminate the filament. However, the model fails to explain the

observed characteristic diameter of the filaments.[3,15] Moreover, the existing calculations[17-19] on self-focusing have not been able to show that a self-focused beam can stabilize into a self-trapped filament (or filaments). The only solution which approximates some kind of stabilization into a self-trapped filament (with the filament diameter weakly oscillating between maxima and minima) is obtained when $\Delta n$ is assumed to be saturable,[17-19] but then the predicted power in the filament is unreasonably high and the predicted filament diameter unreasonably small. In fact, the observed $\Delta n \sim 10^{-3}$ suggests that the unsaturated expression $\Delta n = n_2|E|^2$ may still be a good approximation, even in the filament.

If, somehow by some means, a self-trapped filament with $P = P_{cr}$ and $\Delta n = n_2|E|^2$ were established, it would still be unstable under perturbation. A reduction of power by 1% in the filament would make the filament double its size in a distance of 1 mm through diffraction.[17] Experiments indicate that energy does leak out of the filaments to make exposure of side-view pictures possible. In addition, the various nonlinear optical processes unavoidable in the filament would convert the field energy into heat. In order to sustain the self-trapped filament, external power of the exact amount must be fed into the filament to compensate the power loss.

A different model was later proposed by Lugovoi and co-workers to explain the observed filaments.[21] They pointed out that if the input beam is a pulse, self-focusing should yield a focus (or foci) which moves along the axis.[22] This moving focus appears as a streak (or filament) on the time-integrated photographs. The diameter of the streak is then simply the diameter of the focal spot. This moving

focus model does not depend critically on the assumptions, but avoids the difficulties encountered in the self-trapping model. As we shall see later, it explains essentially all the experimental observations qualitatively, and in some controlled experiments even quantitatively.

To have some feeling on how the focal spot moves in time, we reproduce in Fig. 1 the variation of the focal-spot position in a Kerr liquid as a function of time for a nanosecond input pulse, for which Eq. (12) is assumed to be valid.[28,39,40] (Discussion in picosecond input pulses will be postponed until Section V). However, from the construction of the curve (see the figure caption), we realize that independent of whether Eq. (12) is valid or not the curve shows the following general characteristics, if the medium is sufficiently long. (1) The focal spot first appears inside the medium and immediately splits into two. (2) One moves forward along the upper branch of the curve with a velocity always larger than the light velocity. (3) The other moves along the lower branch of the curve, first backward and then forward. Its forward velocity is always smaller than the light velocity. If the medium is short (less than $z_D$ in Fig. 1), then only the lower branch shows up.

Because of the high laser intensity, stimulated Raman and Brillouin scattering is readily initiated in the focal region along the path of the moving focus. From Fig. 1, it is seen that the wavefront of the backward stimulated radiation should be initiated from the point D on the U curve, where the slope is equal to $-c/n_o$. This backward stimulated radiation initiated around D intercepts the incoming laser beam before the latter self-focuses, and gets amplified under the

latter's expense.[41] Then, if the incoming laser is so highly depleted that it no longer has enough power to self-focus, the lower branch of the U curve gets terminated.[28,42] Also seen from Fig. 1 is that the total amplification of the backward stimulated radiation should depend on both the input pulsewidth and the cell length. In addition to a long cell, the input pulse should be sufficiently long (a few nsec. for a 30 cm cell) in order to have long interaction length for backward stimulated scattering and consequently large total amplification. On the other hand, the upper branch above D should not be affected appreciably by stimulated scattering, since the incoming laser beam is not intercepted and is not appreciably depleted by stimulated scattering before self-focusing.

From the above discussion, we recognize that the moving focus model is far more definite than the self-trapping model. We shall see in the next section that with the moving focus model, quantitative comparison between theory and experiments is now possible if the experiments are performed under controlled input conditions. With the self-trapping model, predictions tend to be at best qualitative.

## III. EXPERIMENTS AND INTERPRETATIONS

In this section, we shall limit our discussion to self-focusing of nanosecond input laser pulses in Kerr liquids. We shall first describe the experiments we have performed under controlled input conditions, and show that the results agree well with the moving focus model. We shall then discuss the earlier experimental results reported in the literature and show that they are consistent with the moving focus model.

## A. Experiments Under Controlled Input Conditions

### 1. General Description of the Experimental Apparatus

In most of our experiments, a single-mode Q-switched ruby laser was used. A pinhole of about 1 mm in diameter was inserted in the laser cavity to insure spatial homogeneity of the output beam. The laser was Q-switched by cryptocyanine in methanol. The output was a smooth pulse with a duration of about 8-nsec. full width at half maximum. The corresponding spectral width was less than 0.01 $cm^{-1}$, as measured by a Fabry-Perot interferometer. The maximum peak power of the laser pulse was about 200 KW.

The advantage of having a single-mode laser for the experiments is obvious. When the laser beam was sent into a cell of $CS_2$ or toluene, instead of tens or hundreds of filaments,[12-15] only one filament was observed in the self-focused beam. It was then possible for us to study the properties of the filament as a function of the input conditions, rather than the average properties of many filaments.

For the detection of pulses, we used an ITT F-4018 fast photodiode in combination with a Tektronix 519 oscilloscope. The overall time constant of such a detector system was about 0.4 nsec. We found that for accurate pulse measurements it was necessary to calibrate the linearity of the oscilloscope.

### 2. Characteristics of Small-Scale Filaments

In all our experiments, Kerr liquids were used as the self-focusing medium. To observe the filaments, we took magnified (100×) pictures of the beam profile at the end of the liquid cell. The film used was either Polaroid Type 47 or Kodak Royal Pan Sheet film from which

densitometer traces can be obtained to measure the sizes of filaments. We first investigated how the beam cross-section at the end of the cell varies with the input laser power for a constant cell length. Experimentally, we define the self-focusing threshold as the power at which stimulated Raman or Brillouin radiation generated in the self-focused beam has reached a detectable level. We found that when the peak power of the input pulse is below threshold, the beam cross-section was roughly the size of the input beam (~ 750 μ). At threshold, a bright spot of about 50 μ in diameter appeared. Then, slightly above threshold, the beam quickly shrank to a more or less limiting size, which seems to be a characteristic of the medium. Further increase of the input power did not change the size, but the energy content in the bright dot appeared to decrease. This energy content was measured by a calibrated photodetector and calibrated photographic technique. It was found to be about 30 ergs for toluene and 8 ergs for $CS_2$, with an energy density of about 4 joules/cm$^2$. Such a high energy density, compared with the energy density of 0.4 joule/cm$^2$ of the laser pulse, was the reason why even without blocking the background light the filament dot could still show up so clearly on the end-view picture.

Similar results were obtained if we kept the input laser power constant, but gradually increased the cell length. After the beam had shrunk to the limiting size, further increase of the cell length only decreased the energy content in the bright dot. However, in a very long cell (> 100 cm), the filament seemed to disappear.

In each liquid, the filament has a characteristic limiting size. Figure 2 shows a typical densitometer trace of the radial profile of

a filament in $CS_2$, from which we measure a filament diameter of 5.6 μm (full width at half maximum). We found from our measurements that the limiting diameter of filaments in $CS_2$, toluene, and nitrobenzene were 5 ± 1 mμ, 10 ± 2 mμ, and 20 ± 2 mμ respectively. The filament diameter seemed to have no temperature dependence. In $CS_2$, it remained unchanged up to the boiling temperature.

In liquid mixtures, the filament diameter varied smoothly from one limiting value to the other as the composition of the mixtures changed from one limit to the other. A typical example is shown in Fig. 3 for mixtures of $CS_2$ and nitrobenzene.

We also tried to measure the light pulse emitted through diffraction from the filament near the end of the cell. We used the optical arrangement shown in Fig. 4a. Lens $L_1$ imaged the exit plane of the cell E to the plane A. A disk of 1 mm in diameter was inserted just somewhat beyond the focus of $L_1$. It was used to block effectively the non-diffracted laser light. A second magnifying lens $L_2$ after the disk ensured that only light diffracted from the filament within a few cm near the end of the cell could be collected by the detector as shown schematically in Fig. 4b. For example, if we assume that light were uniformly emitted along a filament into a cone of $4 \times 10^{-2}$ rad., then with the setup in Fig. 4a, the percentage of light emitted at a distance d away from E and collected by the detector would be given by the solid curve in Fig. 4c. As a comparison, the dashed curve in Fig. 3c corresponds to the case without the lens $L_2$ and with the detector located at A. With this two-lens system, we found that when the input peak power was below the self-focusing threshold, no light

signal reached the detector. At threshold, a pulse of 1 nsec. or longer appeared. Above threshold, as the input power increased, the pulse duration decreased to about 200 psec. when the filament diameter approached the limiting size, and then continued to shorten to less than 100 psec. with the peak power of the pulse remaining roughly unchanged. Here, the deconvolution technique[43] was used to measure pulse duration less than 1 nsec.

These results on the filament characteristics largely confirmed the earlier results obtained with multimode Q-switched lasers,[12-15] and can be understood from the moving focus model. Below the self-focusing threshold, the results agree quantitatively with the self-focusing theory as shown by Maier et al.[42] Above threshold, self-focusing should continuously reduce the observed beam cross-section appearing at the exit plane, until the focus is formed. The diameter of the focus would depend on the incoming beam power if no other nonlinear process were present during self-focusing. However, because of the high intensity in the focal region, nonlinear processes such as stimulated scattering and multiphoton ionization actually happen. They can stop self-focusing and give the focus a limiting diameter. Therefore, above threshold, the observed beam cross-section should appear to have a limiting size, which essentially corresponds to the size of the moving focus or the size of the filament. At very long cell length, the beam power which leads to self-focusing at the end of the cell is very close to the critical power for self-trapping. We then expect that self-focusing at a long distance should be more gradual and more susceptible to the influence of other nonlinear processes. Consequently, the diameter of

the focal spot near the end of the long cell can become much larger. Since the observed filament corresponds to the streak described by the moving focus with the constant limiting diameter, it would seem to have disappeared near the end of the long cell.

We notice from Fig. 1 that just above the self-focusing threshold, the cell length is only slightly larger than the minimum self-focusing distance $z_B$, and the moving focus spends a relatively long time at the end of the cell, leading to the observation of the brightest filament dot and the relatively long filament pulse. For longer cells or higher input peak power, the moving focus then spends less time at the end of the cell. The filament pulse duration and hence the brightness of the observed filament dot should decrease accordingly as we have observed.[44] Here, no quantitative correlation between theory and experiments is attempted, since stimulated scattering affected the observed filament properties and complicated the problem.

So far, there has been no reasonable calculation on the dimension of the moving focus. From the experimental observations on the filament sizes in liquid mixtures, we can conclude that the geometric parameters of the focus should depend on the linear and nonlinear refractive indices of the medium. They may also weakly depend on the parameters of the input laser beam, but we have not yet found conclusive evidence.

We also measured the spectrum of light emitted from the filament, but we shall postpone the discussion to a later section. More observations on the filament properties in connection with stimulated Raman and Brillouin scattering will also be discussed in a later section. We also tried to take the side-view picture of the filament, but our attempt was not successful. It could be that the intensity of the scattered radiation from the filament was too weak to be seen in our case.[13,14]

The above discussion shows that the moving focus model is able to give a natural description of the observed filament, in contrast to the self-trapping model.[1-3] We shall now see that more definite evidences of a moving focus can be obtained in some controlled experiments.

## 3. Evidences of a Moving Focus

The first indication of the existence of a moving focus came from the observation of a bubble of about 100 μ in diameter initiated from the filament at the end of the cell when and only when the cell length was about equal to the minimum self-focusing distance.[28] It would take a few ergs to create such a bubble by vaporization of toluene, and therefore it would require a focus with power of 30 KW to stay at a 100 μ local region over 10 psec. As shown in Fig. 1, this would

happen when the focus is moving around the minimum self-focusing distance $z_B$. If the cell length is larger than $z_B$, then as we mentioned earlier, self-focusing is terminated by the backward stimulated scattering before the focus reaches $z_B$. Consequently, no bubble can be observed at $z_B$.

If the moving focus model is correct, we should expect to see a clear image of the focus by focusing the camera on a plane inside the cell. On the other hand, for a self-trapped filament, we should expect to see a blurred defocused image of the fialemnt. Photographs taken by focusing the camera into the cell at a few cm from the exit window supported the moving focus model. The image of the focus was, however, not as bright as that at the end of the cell. This was believed to be due to depletion by stimulated scattering in the focal region. The above experiment was performed in a 33 -cm. toluene cell, with a laser beam of 750 μm in diameter and a peak power of 200 KW, so that according to Eq. (10), the focus should first appear at the end of the cell and move backward.

We tried the same experiment with the laser beam diameter telescoped down to 300 μm, so that towards the end of the cell, the focus would move in the forward direction according to Eq. (10). We found no clear image of the laser focus when the camera was focused into the cell. There were two possible explanations. The self-focused light after passing through the focal region could be trapped in the dielectric waveguide created by the moving focus.[29,45] Alternatively, the laser light at the focus could be converted into Raman radiation at such a high rate that little was left to be detected on the

photographs over the background.

To see whether it was due to trapping, we inserted a 1-mm glass slide into the cell at 2 or 3 mm apart from the exit window. This glass slide should be effective in breaking a trapped filament through diffraction. If light was indeed trapped in a filament much longer than 2 mm, then insertion of the glass slide would drastically reduce the brightness of the filament image at the exit window unless the diffracted light from the glass slide could be refocused in a 2-mm distance. Our experiments showed that the image at the exit window was not appreciably affected by the insertion of the glass slide. Furthermore, a clear image of the focus was observed when the camera was focused on the entrance side of the glass slide, ruling out the possibility of refocusing of the diffracted light (since refocusing would distort the image of the focus). We therefore concluded that there was no substantial trapping in the filament.

We then suspected that laser light passing through the focus was largely converted to forward and backward Raman radiation. The forward Raman radiation should appear diffracted from the focal region. By focusing the camera into the cell, we found indeed a clear image of the focus at the Raman frequency. Since we expected that the Raman light should be generated all along the path of the moving focus, if we arrange the optical system in Figs. 4 so as to detect light emitted from a longer section of the filament, we should find a Raman pulse of longer duration. Experimental results showed that it was indeed the case.

We also rearranged the optical system in Fig. 4 such that the

detector could collect laser light emitted along the filament over ~ 15 cm from the exit window. At the self-focusing threshold, we found the same relatively long pulse we mentioned earlier. This was expected since the focal spot should not appear far from the exit window. However, at sufficiently high input power, another short pulse, in addition to the first pulse coming from the region near the exit window was observed, with a time delay of a few tenths of a nanosecond between the two. From Eq. (12) and from the measured time delay, we realized that the second pulse must have come from the region where the focus should be moving backward. This was just the region where a clear image of the focus was observed with the camera focused into the cell. Between this region and the region near the exit window, the laser light must have been largely converted to Raman light at the focus.

One may ask why the Raman conversion was more efficient when the focus is moving forward. It is possible that the longitudinal dimension of the moving focus may vary with the focal-spot movement. For example, diffraction of light from a focal spot should be more gradual if diffracted light sees a longer dielectric channel established in front of it by the focus that appeared earlier.[29,45] Thus, the effective focal region could be longer for the forward moving focus, and consequently, the Raman conversion is higher. At the exit window, Raman conversion is limited since the window intercepts the focal spot, and hence the focus is observable at the laser frequency. No theoretical calculation is yet available for such an argument.

All the above experimental results support strongly the moving

focus model. They would be very difficult to be explained by the self-trapping model. However, these experiments all tend to be qualitative. In order to be more convincing, we must demonstrate the focal-spot movement directly and quantitatively. For this purpose, we performed a time-of-flight experiment on the moving focus.

The input laser beam we used for this experiment had a diameter of 300 μ and a peak power of 100 KW. Using the method of Wang,[10] we found experimentally, for this beam propagating in toluene $K/P_o^{1/2} = 4.33$ cm and $P_o = 30$ KW in Eq. (12). Knowing $K/P_o^{1/2}$, and $P(t)/P_o$ for a given input pulse, we then plotted the corresponding U curve for the moving focus as shown in Fig. 5.

For the time-of-flight measurements, we used a 36-cm toluene cell, and inserted a beam splitter (an anti-reflection coated microslide of 100 μm thick) in the cell at a distance d from the window. We wanted to see whether the time at which the focus arrived at d with respect to the focus at the exit window was correctly predicted by the curve in Fig. 5. The experimental setup was also shown in Fig. 5. Focal spots of about 10 μm in diameter were observed both at the beam splitter and at the exit window. The diffracted light from both focal spots was collected with appropriate optical delay by the same fast photodiode, and two pulses with duration less than 0.1 nsec. showed up on the oscilloscope. The time difference between the two pulses can be measured to within an accuracy of 0.08 nsec. The input laser pulse was also monitored simultaneously by a separate fast detection system.

We found that for d = 6.5 cm. and 15 cm., the time delays $\Delta t$ between the two pulses were 0.08 nsec. and 0.25 nsec. respectively.

These measured time delays agree well with the predicted values obtained from the U curve as shown in Fig. 5. If the two pulses had come from a short light pulse propagating with velocity of light in a trapped filament, we would have found $\Delta t = 0.32$ nsec. and 0.75 nsec. respectively for the two cases. Therefore, this experiment proved quantitatively that the moving focus model gave the correct description of the filament. It also showed that the forward moving focus indeed traveled faster than light.

We did not manage to obtain more data points in this experiment because we were afraid that insertion of many beam splitters in the liquid cell might affect self-focusing of the beam and the intensity fluctuations of the laser pulses from shot to shot were normally larger than a few percent. In the next section, we shall describe another time-of-flight experiment. There, many data points were taken to show the full agreement between theory and experiment.

4. Correlation Between Self-Focusing and Stimulated Scattering

It has been known for a long time that stimulated Raman and Brillouin scattering in a Kerr liquid is initiated by self-focusing.[7-9] However, little detail is understood, because of our limited knowledge on the small-scale filaments.

We have performed experiments to correlate, as much as we can, the generation of stimulated Raman and Brillouin radiation with the filament formation through self-focusing. In one of the experiments, we simultaneously monitored the input laser pulse, the laser and the Raman-Stokes pulses diffracted from the axial region within ~ 2 cm from the exit window, the backward Raman-Stokes and Brillouin pulses, and the image of the beam cross-section at the exit window. The

experimental setup is shown in Fig. 6. The Kerr liquid used in this case was toluene.

With the input laser power increasing from below to above the self-focusing threshold, the following sequence of information was obtained. A typical set of data is shown in Fig. 7.

(a) Below the self-focusing threshold, no stimulated Raman and Brillouin scattering was detectable (by our earlier definition) (Fig. 7a).

(b) At the self-focusing threshold, the beam diameter reduced to about 50 μm; the diffracted laser pulse had a duration of about 1 nsec; the backward Brillouin pulse appeared, but both forward and backward Raman radiation was below the detectable level (Fig. 7b).

(c) Slightly above threshold, the beam diameter reduced to within a factor of 2 of the limiting size (~ 10 μm); the duration of the diffracted laser pulse decreased to less than 1 nsec; the backward Brillouin pulse remained nearly unchanged; the backward Raman pulse now appeared, while the forward Raman pulse, though also present, was very weak by comparison (Fig. 7c).

(d) With higher input power, the beam shrank to its limiting size; the duration of the laser pulse diffracted from the filament reduced to about 200 psec; the forward Raman pulses became much stronger, while the backward Raman and Brillouin pulses remained roughly the same (Fig. 7d).

(e) Further increase of the input power reduced the duration of the diffracted laser pulse to less than 100 psec without affecting the limiting size of the filament; the energy content in the pulse was about 30 ergs. The stimulated Raman pulses with pulse duration less

than 100 psec. appeared roughly unchanged. The energy contents in the forward and the backward Raman pulses were about 10 ergs and 100 ergs respectively. The backward Brillouin pulse had a longer duration for a higher input power. Typically, it was a few nsec. long with a peak power of about 10 KW (Fig. 7e).

Similar results were obtained by Maier et al.[42] on $CS_2$. These results can also be understood with the moving focus model. Self-focusing initiates both stimulated Raman and stimulated Brillouin scattering. Since the response time of the Raman process is about a few psec., the Raman radiation grows almost instantaneously to its steady-state value. On the other hand, the response time of the Brillouin process is much slower (~ 10 nsec.), and the Brillouin radiation can only grow with a transient gain. Then, as explained by Maier et al.,[42] although the Brillouin build-up is transient, its gain is still large, and the generated Brillouin signal may reach the detection threshold sooner than the Raman signals. In that case, the Raman signal will show up at somewhat higher input power. As mentioned earlier in Section II, the backward Raman radiation has its wavefront initiated from A (or below A if the cell length is shorter than $z_A$) on the U curve in Fig. 1. It intercepts the incoming fresh laser light and gets highly amplified into an ultrashort pulse.[41] However, as seen from Fig. 1, if the input laser power is higher (corresponding to a lower U curve), the active path for the backward Raman amplification will not be any longer, and therefore the backward Raman pulse should remain roughly unchanged. The backward Raman and Brillouin scattering depletes the laser light effectively,

as can be seen by comparing the transmitted laser pulse with the input pulse. A typical example from our experiment is shown in Fig. 8. The forward Raman radiation is generated mainly in the focus all along the axis. The pulse we detected came from the last 2 cm towards the exit window, and therefore at sufficiently high input power, should have a short duration just as the laser filament pulse (light diffracted from the filament near the exit window) and should be nearly independent of the input power. We found that this forward Raman pulse was always coincident in time with the laser filament pulse.

Knowing where the laser filament pulse and the backward Raman pulse come from, we can perform another time-of-flight experiment to check the moving focus model quantitatively.[30] We simply measure the time correlation between the two pulses and compare the result with the prediction obtained from the U curve. The experimental setup is shown in Fig. 9. We detected the two pulses simultaneously by the same fast detector with appropriate optical delay. From the time difference between the two pulses, we could calculate the distance d between the focus and the position of the backward Raman pulse when the focus just reaches the end of the cell. The experimental results are shown in Fig. 10, with d plotted as a function of the input peak power for four different cell lengths. On the other hand, we obtained

---

a U curve for each input laser pulse from Eq. (12) with $z_f$ as a function of $P/P_o$, where $K_o/P_o^{1/2}$ was found experimentally, using the method of Wang,[10] to be 2.8 cm for our laser beam with a diameter of 300μm. From the U curves, we were able to calculate the curves of d as a function of the input peak power for different cell lengths. They are shown as solid curves in Fig. 10.

Figure 10 shows that the quantitative agreement between the experimental data obtained directly from time correlation measurements and the curves calculated from the moving focus model is very good indeed. This proves that the moving focus model correctly describes the observed filament, and in particular, the forward moving focus has a velocity faster than the velocity of light. It also confirms our assertion on the position where the backward Raman pulse should be initiated.

5. Spectral Broadening Induced by a Moving Focus

Spectral broadening of light emitted from a filament was always used as evidence to support the self-trapping model.[23, 46-50] However, in a recent theoretical paper,[45] we showed that because of the appreciable $\Delta n(\underset{\sim}{r},t)$ induced by the moving focus, the self-focused light traversing the medium can acquire a phase modulation which leads to the broadened spectrum.[51] There is more broadening if towards the end of the cell, the velocity of the forward moving focus is closer to the light velocity. Then, after passing through the focus, the defocused light would see the channel of $\Delta n$ moving in front of it, and would therefore be nonlinearly diffracted (or partially trapped) in the channel for some distance.[45]

For the experimental conditions in Fig. 5, the theory predicted a spectral broadening of about 0.5 $cm^{-1}$ for the laser light emitted from the filament at the end of the toluene cell. Such a broadening should be observable since the spectral width of the input laser was only 0.01 $cm^{-1}$. To check this, we used a Fabry-Perot with a free

spectral range of 1 $cm^{-1}$. The experimental arrangement is shown in Fig. 11a. As before, the optical system only allowed light emitted from the filament at the exit window to go into the Fabry-Perot. The results are shown in Fig. 11b. A spectral width of about 0.3 $cm^{-1}$ was seen, and is slightly more for higher input power as predicted.

To see a broadening of the order of 100 $cm^{-1}$, as observed commonly with multimode lasers,[46-49] the theory requires the focus to approach the exit window with a velocity equal to about 1.1 $c/n_o$.[45] With the same laser beam used in Fig. 11 this requires a toluene cell of more than 100 cm long. If, however, the duration of the input laser pulse is reduced to 1.5 nsec., then only a 35-cm cell is needed.

The above prediction was verified by using a weakly mode-locked laser with a single transverse mode.[29] The laser beam had a diameter of 250 μm, and a maximum peak power of 120 KW. The pulse width of each mode-locked pulse was 1.6 nsec. A set of spectra taken with a Jarrel-Ash 1.5-m. Fastie spectrograph is shown in Fig. 12. They corresponded to mode-locked pulses with peak power larger than 100 KW. For lower peak power, the observed broadening was less. This semi-quantitative agreement between theory and experiments on spectral broadening is another strong proof for the moving focus model.

However, each observed spectrum in Fig.12 was in fact a superposition of the spectra of several filaments created consecutively by several pulses in the mode-locked train. This was evident from the oscilloscope traces of the filament pulses (as an example, see Fig. 13). It made quantitative comparison between theory and experiments difficult, since we were unable to separate the contributions of individual

pulses to the spectrum. In order to obtain more meaningful results, one must repeat the experiments by switching out a single pulse in the mode-locked train, so that only a single filament is present. Such an experiment has been performed with results in good agreement with the theoretical predictions.[52]

Most of the experimental results reported in this section were obtained with toluene. We have performed similar experiments on $CS_2$. There was no qualitative difference between the two cases. We can conclude from these results that, at least for nanosecond input pulses the observed small-scale filaments were actually composed of moving foci. We shall see in the following section that the moving focus model can also describe satisfactorily the earlier experimental results on small-scale filaments obtained by others with Q-switched lasers.

B. Interpretations of Earlier Experimental Results

There have been many observations on small-scale filaments reported in the literature. Some of them confirm the moving focus model, but others have been used to support the self-trapping model. We shall now re-examine these experiments and show that the moving focus model can explain at least qualitatively all the observations. In this section, we shall limit our discussion to experiments with nanosecond input pulses.

A number of experiments were performed with a single-mode laser beam which upon self-focusing, gave rise to a single filament.[28-34,41,42,53] The properties of the filaments reported there agreed well with our observations. The few seemingly different observations can be traced back to the difference in the input conditions such as the input beam

cross-section, the input pulse duration, the cell length, etc.

For example, Korobkin et al.[32] observed with a streak camera only the backward motion of the focus. In their experiment, the laser beam had a pulsewidth of 15 nsec., a peak power of 1.5 MW, and a beam diameter of about .25 mm. The medium was a $CS_2$ cell of 10 cm long. Then, according to Eq. (10) and what we discussed in Section IIB, the focus should first appear at the end of the cell and move backward. This is also the case in the experiment of Maier et al.,[41] who used a laser beam with a pulse duration of 15 nsec., a maximum peak power of 1 MW, and a beam diameter of 600 μm in a $CS_2$ cell of 30 cm. As a consequence, their results, from the measurements of correlation between the backward Raman pulse and the filament pulse similar to ours (Section IIIA3), showed that the backward Raman pulse was initiated at the end of the cell, appearing to be quite different from ours.

The experimental results of Maier et al.[42] on the relation between self-focusing and stimulated scattering agree well with our observations. The laser beam used for their experiment had a pulsewidth of 25 nsec., a peak power varying between 50 KW and 150 KW, and a beam diameter of 435 μ. In a $CS_2$ cell of 30 cm long, the moving focus should always appear first at the end of the cell according to Eq. (10). It is easily seen that their results were consistent with the moving focus model (see Sections IIB and IIIA3). They used the peak transmitted laser power to calculate the diameter of the focused beam. This was correct in their case. However, in general, the peak transmitted laser power corresponds closely to the value at which backward stimulated Raman scattering is first initiated (see Fig. 1, remembering that after

the Raman pulse is initiated, the incoming laser power is quickly depleted to a level below $P_{cr}$), and may not be related to the power which determines the diameter of the focused beam.

In most of the earlier experiments, multimode lasers were used.[12-15] Instead of a single filament, tens or even hundreds of filaments were observed in one shot. In some cases, the output of a pulse laser may consist of mainly $TEM_{oo}$ mode with only a few percent admixture of higher-order modes. Such a beam will appear to be diffraction limited for all practical purposes, and in fact for many lower-order nonlinear optical experiments can be taken as $TEM_{oo}$ mode in the analysis without noticeable error. This is, however, not the case for self-focusing study. As shown by Bespalov and Talanov,[20] a beam with a power density F in a nonlinear medium with $n = n_o + n_2|E|^2$ is unstable against spatial intensity fluctuations with a characteristic size

$$\Lambda = \lambda_o \, c^{1/2}/(16\pi n_o^2 n_2 F)^{1/2} \qquad (13)$$

where $\lambda_o$ is the laser wavelength. For $F = 50$ MW/cm$^2$, $n_2 \approx 10^{-11}$ esu, we have $\Lambda \approx 100\mu$m. Therefore, a small hump of this size in the intensity distribution may cause the local part of the beam to self-focus independently of the rest of the beam. In addition, the local intensity may show narrow spikes in time, although the total power of the whole beam has a smooth variation. These are the reasons for the observation of many filaments with an apparently single-mode laser. Recently, Abbi and Mahr[54] have obtained direct evidence of the correlation between filaments and intensity spikes.

With the appearance of many filaments, one would lose all information about the input conditions for the formation of individual filaments. Any quantitative comparison between theory and experiments would then be impossible. However, the qualitative features of the results on filaments can still be described fairly well by the moving focus model.

It was observed that even a Q-switched laser beam yielded filaments with appreciable spectral broadening. This was used as a strong argument for the self-trapping model.[23,46-50] We now understand that in those experiments the laser beam was multimoded, and must have contained narrow spikes of the order of 1 nsec. or less.[54] As we showed in Section III A5, these spikes were responsible for the observed filaments with broadened spectra, but these filaments were actually composed of moving foci.

The experimental results which have most often been used as argument for the self-trapping model are those of Denariez-Roberge and Taran.[23] However, their results can be explained quite satisfactorily by the moving focus model. They found that filaments were still present after the laser beam passed through a screen with 30 μm holes, and the number of filaments decreases by a factor of 3 when a glass slide of 1mm thick was inserted in the liquid at 1.3 cm from the exit window. Since about 50 filaments were observed with a laser beam of 500 μm in diameter in their experiments, it was clearly possible that local intensity humps of 30 μm or less in diameter could go through the holes on the screen and self-focus to form filaments of moving foci after the screen. On the other hand, the small local humps in the beam profile

and the filament already formed would be smoothed out by diffraction in passing through the 1-mm glass slide and would not have enough strength to self-focus into filaments in the rest 1.3 cm distance. Therefore, the number of filaments after the glass slide should decrease. Denariez-Roberge and Taran[23] also showed that the observed spectral broadening increases with the length of a filament. According to the moving focus model (Section IIB), a longer filament corresponds to a higher input laser power or a longer cell length. In both cases, from our analysis on spectral broadening,[45] we should expect to see a broader spectrum. This was confirmed in our recent experiments with weakly mode-locked pulses.[52]

Thus, so far as we know, there has been no experimental results which are inconsistent with the moving focus model, at least for the case of nanosecond input pulses. Some observations[14] on the filaments reported in the literature seemed to be anomalous, but those results were difficult to reproduce quantitatively, and were also difficult to analyze without knowing their input conditions.

## IV. UNSOLVED PROBLEMS OF SMALL-SCALE FILAMENTS

Quite a few technical difficulties exist in the experimental study of self-focusing and small-scale filaments, even for the case of nanosecond input pulses. In order to measure characteristics of self-focusing and filaments, one would like to have in addition to a well-controlled, high-power single-mode laser, detection systems of various forms which have both high sensitivity and fast response time with time-resolving power, hopefully in the picosecond range. While some of them may be available, others are not, as limited by our present-day technology. Consequently, we have not yet been able to obtain quantitative information for all filament properties.

One of the most important properties yet to be measured quantitatively is the duration and pulse shape of the filament pulse emitted from the filament near the exit window. Theoretically, from the moving focus model, this pulse duration in the limit of high input power should be of the order of the relaxation time for molecular reorientation,[45] and if nonlinear diffraction (or partial trapping) of light occurs in the channel of induced refractive index $\Delta n$, the pulse should appear with a longer trailing edge.[45] Measurements of pulse duration and pulse-shape as a function of input laser power and cell length will give us not only another check on the moving focus model, but also information on how the light is diffracted from the focus. In this respect, we would also like to know the angular distribution of the filament pulse. Unfortunately, the filament pulse is weak ($\sim$ 10 ergs), the filament dimension is small ($\sim$ 10 $\mu$m), and hence, with the presently available detection scheme, measurements of the filament pulse duration

have not been able to go below 100 psec.[15,43]

In the experiments on small-scale filaments, it would always be more gratifying if one could observe the whole length of a filament from the side. One would then be able to see how the length of the filament varies with the input power, and which section of the filament has the laser light converted to Raman radiation. This information will also be of great help to the understanding of the problem. In fact, it would be even more desirable if we could observe how the beam profile changes with time over the entire cell length. However, the measurements are extremely difficult. Although side-view pictures of filaments have been taken, such measurements under controlled input conditions have not yet been reported.

We would also like to know $\Delta n(\underset{\sim}{r},t)$ over the entire cell, from which we can map out the field intensity distribution as a function of time and hence, gain information on the dynamics of self-focusing and filament formation. Shimizu and Stoicheff[55] have tried to measure a $\Delta n$ averaged over a transverse cross-section by using a probing beam from the side. Carman et al.[56] have used essentially the same technique in the picosecond case. However, the resolution of their technique in space and time is still low and the accuracy is poor.

Theoretically, there are computational difficulties in the self-focusing problem. In principle, the problem is simple since one only has to solve the wave equation (5) together with the relaxation equation (7) for $\Delta n$. Unfortunately, the solution of such a set of coupled nonlinear differential equations is a major problem even on a

big computer. Calculation of self-focusing in the pre-focus region has been done,[3,18,19,38] but no one has yet been successful in extending the calculation into and beyond the focal region. Such a calculation could give us the dimensions of the moving focus and in particular, the detailed geometry of focusing and diffraction of light in the focal region. From the success of the moving focus model, we can almost be certain that the observed filament size should correspond to the diameter of the moving focus. We also believe that the geometry of focusing and defocusing depends on the input power and the position of the focus.[57] However, it is likely that both the size of the focus and the focusing geometry are the results of interplay between self-focusing and stimulated scattering and other nonlinear processes.

Inclusion of stimulated scattering in the self-focusing calculation will certainly make the calculation even much more complicated, and reasonable approximation must be used before one attempts to solve the set of coupled equations. It would, of course, simplify the problem a great deal if one could suppress the stimulated scattering processes by some appropriate means. The simplest case of self-focusing is probably the case of self-focusing in a monoatomic gas,[58] where $\Delta n$ arises from saturation of the refractive index in the anomalous dispersion region.[59] There, not only stimulated scattering does not occur, but also since $\Delta n$ is an electronic effect, it responds to the field instantaneously. In addition, the focusing does not seem to be as sharp as in the case of liquids.[58] The calculation of self-focusing can therefore be greatly simplified. Another way of suppressing the stimulated scattering processes is to use ultrashort pulses. However,

even with picosecond pulses, one cannot suppress the stimulated Raman scattering completely.[60] As a matter of fact, the picosecond case has additional complications resulting from transient response of $\Delta n$ in the pre-focusing region. It happens that because of the transient response of $\Delta n$, self-focusing of a picosecond pulse is not very sharp,[38] and therefore, complete numerical solution of this picosecond problem should be possible with the available computers.[61] In the next section, we shall discuss only qualitatively the problem of self-focusing of picosecond pulses.

## V. SELF-FOCUSING OF PICOSECOND PULSES

We have shown that we can successfully explain the observed filaments with the moving focus model for the case of nanosecond input pulses. Now, we want to show that by properly modifying the moving focus model, we can also explain the observed filaments in the picosecond case.

The problem of self-focusing of picosecond pulses in Kerr liquids is different from the nanosecond case in two respects. 1) The spatial extent of a picosecond pulse in the propagation direction is only of the order of a mm. 2) The picosecond pulsewidth is of the order of the relaxation time of the orientational Kerr effect, and therefore the field-induced $\Delta n$ due to molecular reorientation cannot respond instantaneously to the varying field. This makes self-focusing of the beam much more gradual.

The major difficulty of this picosecond problem at present is, however, not theoretical but experimental. It is difficult to make a mode-locked laser lase in a single transverse mode. Consequently, in the self-focusing experiments with picosecond mode-locked pulses, one usually observes many filaments in each shot. In addition, because of lack of proper detectors, one cannot obtain detailed quantitative knowledge about the temporal and spatial distribution of a picosecond pulse. Thus, without knowing quantitatively the input conditions, our interpretation of the experimental results can at most be qualitative. This lack of information about the input pulses is also the reason for the apparent differences in the observed characteristics of the filaments reported by different research groups.

Generally speaking, the filaments observed with picosecond pulses are quite similar to those generated by nanosecond pulses. There are many reports on the observation of filaments in Kerr liquids with picosecond pulses.[25,27,56] The results obtained by Svelto and co-workers[25,27] are probably among the best and have been most carefully analyzed. Their results and also those of others[56] show that the filaments have the following general characteristics. 1) The filaments are a few microns in diameter. 2) The filament radiation show large spectral broadening with semi-periodic structure. In some cases, the extent of broadening on the Stokes and the anti-Stokes sides are nearly equal. 3) The spectral broadening appears to have no radial dependence over the main cross-section of a filament. 4) The extent of spectral broadening increases with the input peak power and the length of the liquid medium. Svelto et al.[25,27] used the self-trapping model to explain their results. They showed that for successful interpretation of the results, there should exist a physical mechanism which contributes non-negligibly to $\Delta n$ and has a relaxation time in the sub-picosecond range. They suggested that rocking of molecules could be the mechanism. They also deduced from their analysis other conclusions which, however, appear to be physically unreasonable. In this section, we shall show that their results can also be explained by the modified moving focus model. It is not necessary to introduce rocking of molecules as an important mechanism for $\Delta n$ in Kerr liquids. The unreasonable conclusions can also be avoided.

Theoretically, self-focusing of a picosecond pulse is also governed by the set of Eqs. (7) - (9). If the pulsewidth is comparable with

the Kerr relaxation time $\tau$, then the quasi-steady-state approximation is no longer valid, and self-focusing of the later part of the beam now depends on how the leading part interacts with the medium. While analytical solution of Eqs. (7) - (9) is difficult to obtain, numerical solution has been attempted by Fleck and Kelley,[38] and more recently extended by Shimizu and Courtens.[62] Here, we shall only describe the solution qualitatively.

From Eq. (7), we find $\Delta n(z,\xi) = (1/\tau)\int_{-\infty}^{\xi} \Delta n_o(A^2(z,\eta))e^{-(\xi-\eta)/\tau}d\eta$. Therefore, if the pulsewidth of the input pulse is short or comparable with the relaxation time $\tau$, then propagating in the medium, the last part of the pulse should always see a larger $\Delta n$ and consequently should focus earlier. Thus, we would find that the propagating pulse first gets deformed through self-focusing into a horn shape with the broad face corresponding to the leading edge (see Fig. 14).[62] Because of the transient response of $\Delta n$, this self-focusing is much more gradual compared with the quasi-steady-state case.[38] Then, for the same reason, this horn-shape pulse can travel a long distance in the medium without too much change in its shape.[62,63] In this region, the self-focusing action of the pulse (except the leading edge) is roughly balanced by diffraction. However, since the leading edge keeps on diffracting, the entire horn-shape pulse should eventually diffract accordingly.

Let us look at the propagation of different parts of the pulse separately.[64] The front part sees little $\Delta n$ and therefore keeps on diffracting. The middle part sees a $\Delta n$ induced by the front part. It

first self-focuses and then gradually diffracts as $\Delta n$ decreases following the diffraction of the front part. Because of the relatively small $\Delta n$ it sees, the diameter of the focal spot can be fairly large. Also, because of the transient response of $\Delta n$ and the slow diffraction after focusing, the focal region can be very long as compared to the quasi-steady-state case. Similar description applies to the last part of the pulse except that it sees a larger $\Delta n$ and therefore focuses to a smaller diameter. The focal region can still be extended over many cms.[62] Comparing with the quasi-steady-state case, we realize that the differences are only in the dimensions of the focal region and in the detailed geometry of focusing and diffraction. In the quasi-steady-state case, focusing is much sharper and the longitudinal dimension of the focal region much smaller.

We shall now discuss how the above physical picture can explain the observed characteristics of filaments produced by picosecond pulses. First, as the horn-shape pulse propagates in the medium, the streak described by the neck of the horn corresponds to the filament. Then, as the horn-shape pulse diffracts, the neck of the horn increases in diameter proportionally, and eventually the filament appears to be terminated, as observed by Carmen et al.[56] We recognize that the diameter of the neck should correspond to the diameter of the filament. However, numerical calculations of Shimizu and Courtens[62] indicate that contrary to the experimental observation, the diameter of the neck should depend quite sensitively on the peak power of the input pulse. It is believed that some highly nonlinear optical processes could stop the focusing action and hence limit the diameter of the

focal region.[62] For example, multi-photon ionization could happen in the focal region and regulate the beam diameter.

It is probably more important to explain the observed characteristic spectral broadening. From what we have learned in the nanosecond case, we know that spectral broadening is mainly due to phase modulation, and that the qualitative feature of the semiperiodic broadening does not depend critically on the final pulse shape. We shall be interested only in the spectral broadening of radiation from the filament. As an approximation, we can assume that the phase modulation in the region before the pulse more or less stabilizes into a horn shape can be neglected since $\Delta n$ in this region is relatively small. Then, the overall phase modulation arises simply from the result of the horn-shape pulse propagating in the nonlinear medium. We shall also assume that diffraction of the horn-shape pulse can be neglected. This is true over a limited distance. As we mentioned earlier, at long distances, diffraction becomes appreciable and the filament finally disappears. Although phase modulation may still persist, the spectral intensity should greatly reduce.

To illustrate spectral broadening due to phase modulation in this case, let us assume that the horn-shape pulse propagating in the medium

has the intensity distribution given by $A_o^2 \exp[-\xi^2/t_p^2 - 2r^2/r_o^2(\xi)]$

with $r_o(\xi)/a = 1$ if $\xi \leq t_1$

$= (1-\Delta)e^{-(\xi-t_1)/\tau_1} + \Delta$ if $t_1 \leq \xi \leq t_2$

$= (1-\Delta)e^{-(t_2-t_1)/\tau_1} + \Delta$ if $\xi \geq t_2$

where $t_p$, a, $t_1$, $t_2$, $\tau_1$, and $\Delta$ are constant coefficients. We choose, as an example, $t_p = 1.25\ \tau$, $t_1 = 2.5\ \tau$, $t_2 = 2\tau$, $\tau_1 = \tau$, and $\Delta = 0.05$, with $\tau$ taken to be 2 psec for $CS_2$. We also assume $A_o^2/(2n_2/n_o)k^2a^2 = 40$. These values are chosen to approximate the calculations in Fig. 1 of Ref. 38. From the given intensity distribution $A^2(\xi,z)$, we can calculate $\Delta n(\xi,z)$ from Eq. (7) by assuming $\Delta n_o = n_2 A^2$. From Eq. (9), we find at $r = 0$,

$$\partial s(\xi,z)/\partial z = (\Delta n/n_o) - (2/k^2 r_o^2(\xi)) \qquad (14)$$

from which we obtain $s(\xi,z) \approx (\partial s/\partial z)z$. Knowing $A^2$ and s, we can then calculate from Fourier transform the corresponding spectral distribution. The results for $z = 0.15\ ka^2$ are shown in Fig. 15.

The spectrum in Fig. 15 has indeed the semiperiodic structure with Stokes and anti-Stokes broadening nearly equal, although the Stokes side is more intense. This agrees with the experimental observation.[25,27,56] Numerical calculations of Shimizu and Courtens[62] yield a similar spectrum. We realize from Fig. 15 that only the neck portions of the horn-shape pulse is responsible for the anti-Stokes broadening while the rest of the pulse is responsible for the Stokes

broadening. The Stokes-anti-Stokes symmetry in the present case arises from the fact that the time dependence in $\Delta\phi = ks$ comes solely from the time dependence in $\Delta n_{eff}/n_o \equiv (\Delta n/n_o) - (2/k^2 r_o^2)$, and that the fast reduction of $r_o$ near the end of the pulse makes rise and fall of $\Delta n$ appear more symmetric. Withoutthe diffraction term $(2/k^2 r_o^2)$, we would find $\Delta n_{eff}$ more asymmetric because of the relaxation of $\Delta n$. This is quite different from the nanosecond case. There, because of the rapid motion of the sharp focal spot, the time dependence in $\Delta\phi$ is mainly due to the change of the effective integration length with time.[45,52] Consequently, with or without the diffraction term $(2/k^2 r_o^2)$, the Stokes-anti-Stokes asymmetry remains nearly the same. If in the picosecond case, the pulsewidth is either much longer or much shorter than the relaxation time $\tau$, then the $\Delta n_{eff}$ appears less symmetric and the anti-Stokes broadening would be less than the Stokes broadening. As seen from Eq. (14), the phase modulation, and hence the spectral broadening, should increase with the distance the horn-shape pulse travels or with the peak power of the input pulse.

In the above discussion, we have neglected the dispersive effect of the medium. Dispersion may be important if spectral broadening extends beyond several hundred $cm^{-1}$.[65] However, we believe that it will not change the qualitative feature of the spectral broadening appreciably.

We can also find the broadened spectrum at $r \neq 0$ from a similar calculation. Since the horn-shape pulse is supposed to propagate a long distance without too much change in its shape, the phase function s should be nearly independent of r. This is particularly true for very

small r. Therefore, we expect to find little radial dependence in the spectral broadening of the filament. Detailed numerical calculations of Shimizu and Courtens[62] lead to the same conclusion. This was actually observed experimentally, and was pointed out emphatically by Cubbedu et al.[27] In Eq. (9), the weak dependence of s on r at small r means that the radial dependence of the $\Delta n$ term is nearly cancelled by that of the diffraction term at small r.

Cubbedu et al.[25,27] used the self-trapping model to explain their results. Here, a self-trapped filament corresponds to a short pulse of constant diameter propagating in the medium. In order to explain the observation that the spectral broadening of a filament is independent of r, they arrived at the conclusion that $\Delta n$ must have the form $\Delta n = \Delta n_1 (r) + \Delta n_2(z,t)$. The appearance of the time-independent $\Delta n_1$ is, however, a direct consequence of their assumption of a self-trapped filament. The second part $\Delta n_2$ depending on the field intensity was responsible for the phase modulation and hence the spectral broadening. This separation of $\Delta n$ into two parts appears rather unnatural and contradicts our physical intuition. As we have seen, the above conclusion can be avoided in our model. Cubbedu et al.[27] derived the values of $\Delta n_1$ and $\Delta n_2$ from their spectral broadening data using the self-trapping model and Eq. (9), but were not able to explain the existence of $\Delta n_1$ which appeared even before the pulse was present in the medium in their analysis. In fact, their spectral analysis, if properly done, only allows them to deduce $\Delta n$ to within a time-independent constant, and hence $\Delta n_1(r)$ is indeterminable from the experimental spectra in their model.

Polloni et al.[25] argued that from the maximum extent of the anti-Stokes broadening $\nu_{as}$ and the number of minima m in the anti-Stokes side of the spectrum, one can set an upper limit equal to $m/\nu_{as}$ for the relaxation time $\tau$. Since their experimental data showed $m/\nu_{as}$ in the subpicosecond range, they suggested that vibration or rocking of molecules may be the physical mechanism responsible for the spectral broadening. This is however not quite true. First from Eq. (9), we realize that $m/\nu_{as}$ is actually the upper limit of the fall time of s which should appear to decay faster than $\Delta n$ because of the effect of diffraction. Then, more importantly, one should not expect to see all the minima in a spectrum clearly separated. It is possible that in the actual spectrum, several peaks are lumped together to form a broad peak. For example, if $d\Delta\phi/dt$ remains roughly constant around $(d\Delta\phi/dt)_{max}$ while $\Delta\phi = ks$ changes over $6\pi$, then the last peak in the spectrum is actually the superposition of four individual peaks. Therefore, the total number of minima m observed is always less than the actual number of minima $m_o$ given by $\sim (\Delta\phi)_{max}/2\pi$ where $(\Delta\phi)_{max}$ is the maximum phase change. Then, we must use $m_o/\nu_{as}$ instead of $m/\nu_{as}$ as the upper limit of the relaxation time. Since $m_o > m$, this upper limit can be longer than the one given by Polloni et al.[25] However, without knowing the detailed variation of $\Delta\phi(t)$, it is not possible to estimate the value of $m_o$.

Because of the transient response of $\Delta n$, the threshold intensity for generation of filaments in the picosecond case is much higher than that in the nanosecond case. Then, according to Eq. (13) shown by Bespalov and Talanov,[20] the beam should be more unstable against spatial/intensity fluctuations and consequently, it is more likely to generate many filaments if the beam does not have a perfect $TEM_{oo}$ mode. Experimentally, one usually finds several or many filaments in each shot when the picosecond mode-locked pulses are used.

From what we have discussed, we can conclude that the modified moving focus model can indeed explain successfully the experimental results of filaments generated by a picosecond pulse. More quantitative interpretation should come from the numerical solution of Eqs. (7) - (9) with appropriate input conditions, as has been attempted by Shimizu and Courtens.[62] However, in the calculations, it is also important to incorporate the appropriate nonlinear processes which control the final geometry of focusing. It is of course more important to have controllable experiments on filaments in the picosecond case. Without knowing exactly the input conditions in the experiments, the results can at most be interpreted qualitatively.

Finally, we should discuss briefly self-focusing of a picosecond pulse in a medium where electronic contribution to nonlinearity is dominant. This has been the subject of many experimental reports,[24,26,65] all of which have used the self-trapping model to explain the observations. However, from our previous discussion, it is clear that the moving focus model should be more appropriate for this case. In fact, since the

electronic relaxation time is of the order of $10^{-15}$ sec., which is much shorter than a picosecond, the quasi-steady-state approximation of self-focusing applies here. We can therefore again draw a U curve to describe the moving focus, but the width of the U curve is only a few picoseconds. As we mentioned earlier,[29,45] the output filament pulse should have a characteristic width of the order of the relaxation time, and hence in the present case, it should have a width of about $10^{-15}$ sec. This is the shortest optical pulse one can generate in any nonlinear optical experiment. Because of the short filament pulsewidth, the corresponding spectrum should have a large smeared broadening, while broadening due to phase modulation becomes less important. Experimentally, no clear semi-periodic structure was observed in the broadened spectrum.[26]

## VI. CONCLUSIONS

We have shown that the moving focus model gives a natural description of the small-scale filaments generated by laser pulses in nonlinear media. The model explains qualitatively all the previously reported experimental results on filaments. However, we realize that in order to prove definitely the moving focus model, we must know the input conditions of the experiments. Only then, the results can be subject to detailed analysis. Controlled experiments with known input conditions have been carried out with single-mode Q-switched pulses. The results are very well explained by the moving focus model. In some cases, even quantitative agreement between theory and experiments have been obtained. We can therefore conclude that moving foci are indeed responsible for the observed small-scale filaments. The moving focus model, properly modified, can also explain the observed filaments generated by picosecond pulses. In this case, however, because of the transient response of $\Delta n$, focusing and diffraction are very gradual, and the dimensions of the focal regions for different parts of the pulse can be very different. As a result, the pulse appears to stabilize through self-focusing into a horn shape and propagate over many centimeters without too much change in its shape. We show that in order to explain the observed broadened spectra, it is not necessary to assume molecular libration as an important mechanism for $\Delta n$ as suggested by Polloni et al.[25] We have also briefly discussed the many unsolved problems related to self-focusing and small-scale filaments.

## ACKNOWLEDGEMENT

This work was performed under the auspices of the U. S. Atomic Energy Commission.

† IBM Fellow;
Permanent address: IBM Research Center, P.O. Box 218, Yorktown Heights, N.Y. 10598

1. G. A. Askar'yan, Zh. Eksp. i Teor. Fiz. 42, 1567 (1962) [English translation: Soviet Phys. JETP 15, 1088 (1962)].
2. V. I. Talanov, Izv. Vuzov (Radiofizika) 7, 564 (1964) [English translation: Radiophysics 7, 254 (1964)].
3. R. Y. Chiao, E. Garmire, and C. H. Townes, Phys. Rev. Letters 13, 479 (1964). In this paper, the word "filament" does not mean a self-trapped filament, but refers to the intense streaks observed in experiments.
4. P. L. Kelley, Phys. Rev. Letters 15, 1005 (1965).
5. V. I. Talanov, ZHETF Pis. Red. 2, 218 (1965) [English translation: JETP Lett. 2, 138 (1965)].
6. S. K. Akhmanov, A. P. Sukhorukov, and R. V. Khokhlov, Zh. Eksp. Teor. Fiz. 50, 1537 (1966) [English translation: Soviet Phys. JETP 23, 1025 (1966)].
7. N. E. Pilipetskii and A. R. Rustamov, ZhETF Pis. Red. 2, 88 (1965) [English translation: JETP Lett. 2, 55 (1965)]; G. Hauchecorne and G. Mayer, Compt. Rend. 261, 4014 (1965).
8. Y. R. Shen and Y. J. Shaham, Phys. Rev. Letters 15, 1008 (1965); Phys. Rev. 163, 224 (1967).
9. P. Lallemand and N. Bloembergen, Phys. Rev. Letters 15, 1010 (1965).
10. C. C. Wang, Phys. Rev. Letters 16, 344 (1966); Phys. Rev. 152, 149 (1966).
11. E. Garmire, R. Y. Chiao, and C. H. Townes, Phys. Rev. Letters 16, 347 (1966).
12. R. Y. Chiao, M. A. Johnson, S. Krinsky, H. A. Smith, C. H. Townes, and E. Garmire, IEEE J. Quantum Electron. QE-2, 467 (1966).

13. R. G. Brewer and J. R. Lifsitz, Phys. Letters 23, 79 (1966).

14. R. G. Brewer and C. H. Townes, Phys. Rev. Letters 18, 196 (1967).

15. R. G. Brewer, J. R. Lifsitz, E. Garmire, R. Y. Chiao, and C. H. Townes, Phys. Rev. 166, 326 (1968).

16. T. K. Gustafson, P. L. Kelley, R. Y. Chiao, and R. G. Brewer, Appl. Phys. Letters 12, 165 (1968).

17. W. G. Wagner, H. A. Haus, and J. H. Marburger, Phys. Rev. 175, 256 (1968).

18. V. N. Goldberg, V. I. Talanov, and R. E. Erm, Izv. Vysshikh Uchebn. Zavedenii Radiofiz. 10, 674 (1967).

19. J. H. Marburger and E. L. Dawes, Phys. Rev. Letters 21, 556 (1968); E. L. Dawes and J. H. Marburger, Phys. Rev. 179, 862 (1969).

20. V. I. Bespalov and V. I. Talanov, ZhETF Pis. Red. 3, 471 (1966) [English translation: JETP Letters 3, 307 (1966)].

21. V. N. Lugovoi and A. M. Prokhorov, ZhETF Pis. Red. 7, 153 (1968) [English translation: JETP Letters 7, 117 (1968)].
A. L. Dyohko, V. N. Lugovoi, and A. M. Prokhorov, ibid. 6, 655 (1967) [English translation: JETP Letters 6, 146 (1967)].
V. N. Lugovoi, Dokl. Akad. Nauk SSSR 176, 58 (1967) [English translation: Soviet Phys. Doklady 12, 866 (1968)].

22. J. H. Marburger and W. G. Wagner, IEEE J. Quantum Electron. QE-3, 415 (1967).

23. M. M. Denariez-Roberge and J-P. E. Taran, Appl. Phys. Letters 14, 205 (1969).

24. R. G. Brewer and C. H. Lee, Phys. Rev. Letters 21, 267 (1968).

25. R. Polloni, C. A. Sacchi, and O. Svelto, Phys. Rev. Letters 23, 690 (1969);
R. Cubeddu, R. Polloni, C. A. Sacchi, and O. Svelto, Phys. Rev. A2, 1955 (1970).

26. R. R. Alfano and S. L. Shapiro, Phys. Rev. Letters 24, 1217 (1970).

27. R. Cubeddu, R. Polloni, C. A. Sacchi, O. Svelto, and F. Zaraga, Phys. Rev. Letters 26, 1009 (1971); Optics Comm. 3, 310 (1971).

28. M. M. T. Loy and Y. R. Shen, Phys. Rev. Letters 22, 994 (1969).

29. M. M. T. Loy and Y. R. Shen, Phys. Rev. Letters 25, 1333 (1970).

30. M. M. T. Loy and Y. R. Shen, Appl. Phys. Letters 19, 285 (1971).

31. G. M. Zverev, E. K. Maldutis, and V. A. Pashkov, ZhETF Pis. Red. 9, 108 (1969) [English translation: JETP Letters 9, 61 (1970)];
G. M. Zverev and V. A. Pashkov, Zh. Eksp. Teor. Fiz. 57, 1128 (1969) [English translation: Sov. Phys. JETP 30, 616 (1970)].

32. V. V. Korobkin, A. M. Prokhorov, R. V. Serov, and M. Ya. Shchelev, ZhETF Pis. Red. 11, 153 (1970) [English translation: JETP Letters 11, 94 (1970)].

33. N. I. Lipatov, A. A. Manenkov, and A. M. Prokhorov, ZhETF Pis. Red. 11, 444 (1970) [English translation: JETP Letters 11, 300 (1970).

34. C. R. Giuliano and J. H. Marburger, Phys. Rev. Letters 27, 905 (1971).

35. Y. R. Shen, Phys. Letters 20, 378 (1966).

36. P. Debye, Polar Molecules (Dover Publications, New York, 1945), chapter 5.

37. S. A. Akhmanov, A. P. Sukhorukov, and R. V. Khokhlov, Usp. Fiz. Nauk 93, 19 (1967) [English translation: Soviet Phys. Uspekhi 10, 609 (1968)].

38. J. A. Fleck and P. L. Kelley, Appl. Phys. Letters 15, 313 (1969).

39. A. A. Abramov, V. N. Lugovoi, and A. M. Prokhorov, ZhETF Pis. Red. 9, 675 (1969) [English translation: JETP Letters 9, 419 (1969)].

40. T. K. Gustafson and J-P.E. Taran, IEEE J. Quantum Electron. QE-5, 381 (1970).

41. M. Maier, W. Kaiser, and J. A. Giordmaine, Phys. Rev. Letters 17, 1275 (1966); Phys. Rev. 177, 580 (1969).

42. M. Maier, G. Wendl, and W. Kaiser, Phys. Rev. Letters 24, 352 (1970).

43. M. M. T. Loy and Y. R. Shen, Appl. Phys. Letters 14, 380 (1969).

44. A short pulse of less than 100 psec. long can be created from a Q-switch input pulse by this process. Self-focusing as a sharpening mechanism was first discussed in Ref. 22 and observed by G. L. McAllister, J. H. Marburger, and L. G. DeShazer, Phys. Rev. Letters 21, 1648 (1968).

45. Y. R. Shen and M. M. T. Loy, Phys. Rev. A3, 2099 (1971); (first presented at the Sixth International Quantum Electronics Conference at Kyoto, Japan, September 1970).

46. R. G. Brewer, Phys. Rev. Letters 19, 8 (1967).

47. F. Shimizu, Phys. Rev. Letters 19, 1097 (1967).

48. A. C. Cheung, D. M. Rank, R. Y. Chiao, and C. H. Townes, Phys. Rev. Letters 20, 786 (1968).

49. J. R. Lifsitz and H. P. H. Grieneisen, Appl. Phys. Letters 13, 245 (1968).

50. T. K. Gustafson, J-P. E. Taran, H. A. Haus, J. R. Lifsitz, and P. L. Kelley, Phys. Rev. 177, 306 (1969).

51. In Ref. 45, the quantity $\Delta n$ in Eqs. (4), (5), and (6) should be replaced by $\Delta n_{eff} = \Delta n - 2n_o/k^2 r_o^2(z,\xi)$. See Eq. (14) in the text. Inclusion of the diffraction term $2n_o/k^2 r_o^2$ in $\Delta n_{eff}$ does not affect the semi-quantitative discussions in Ref. 45.

52. George K. L. Wang and Y. R. Shen, (to be published).

53. V. V. Korobkin and R. V. Serov, ZhETP Pis. Red. 6, 642 (1967) [English translation: JETP Letters 6, 135 (1967)].

54. S. C. Abbi and H. Mahr, Phys. Rev. Letters 26, 604 (1971).

55. F. Shimizu and B. P. Stoicheff, IEEE J. Quantum Electron. QE-5, 544 (1969).

56. R. L. Carmen, J. Reintjes and F. Shimizu, Abstracts for Sixth International Quantum Electronic Conference, (Kyoto, Japan, 1970) Paper 9-4 ; J. Reintjes, F. Shimizu, and R. L. Carman, Bull. Am. Phys. Soc. 16, 71 (1971).

57. The longitudinal dimension of the focus is probably longer for a focus at a larger distance away, since it would be infinitely long if the focus is at infinity.

58. D. Grischkowsky, Phys. Rev. Letters 24, 866 (1970).

59. A. Javan and P. L. Kelley, IEEE J. Quantum Electron. QE-2, 470 (1966).

60. R. L. Carman, F. Shimizu, C. S. Wang, and N. Bloembergen, Phys. Rev. A2, 60 (1970) and the references therein.

61. J. A. Fleck (private communication).

62. F. Shimizu and E. Courtens, paper presented at the Esfahan Symposium on Fundamental and Applied Laser Physics, Iran, August 1971.

63. S. A. Akhmanov, A. P. Sukhorukov, and R. V. Khokhlov, Zh. Eksp. Teor. Fiz. 51, 296 (1966) [English translation: Sov. Phys. JETP 24, 198 (1967)].

64. In principle, we can also draw a U curve in this case to describe the position of the foci of the beams entering the medium at various times during the pulse. However, the U curve is not very meaningful here since the foci of beams from different parts of the pulse have very different dimensions and they are usually very long and not very well defined.

65. N. Bloembergen, paper presented at the Esfahan Symposium on Fundamental and Applied Laser Physics, Iran, August 1971.

66. J. P. McTague, C. H. Lin, T. K. Gustafson, and R. Y. Chiao, Phys. Letters 32A, 82 (1970).

FIGURE CAPTIONS

Fig. 1. Lower trace describes the input power P(t) as a function of time t. Peak power is 42.5 kW and the half-width at the $e^{-1}$ point is 1 nsec. Upper trace, calculated from Eq. (12), describes the position of the focal spot as a function of time. Values of $P_o$ and K used are 8 kW and 11.6 cm-$(kW)^{1/2}$, respectively, which correspond roughly to an input beam of 400 μ in diameter propagating in $CS_2$. The dotted lines, with the slope equal to the light velocity in $CS_2$, indicate how the light propagates in the medium along the z axis at various times.

Fig. 2. Densitometer trace of a filament in $CS_2$.

Fig. 3. Average diameter of a filament in $CS_2$-nitrobenzene mixture. The diameter is obtained from the width at half maxima of the densitometer trace of a filament. Each point on the curve is an average of five measurements.

Fig. 4. (a) Experimental setup to measure radiation from the filament, near the end of the cell. The unfocused and the non-divergent background light is blocked by a small disk at D. ($L_1$, $L_2$, converging lenses; E, exit plane of the cell; A, image plane of E; B, detector.)

(b) Schematic drawing to show that the setup discriminates against diverging light from deep inside the cell.

(c) Percentage of light reaching the detector from a source inside the cell at a distance d away from E. The distances from E to $L_1$, from $L_1$ to $L_2$, and from $L_2$ to B are 11.5, 24.5, and 41 cm respectively. The focal lengths of $L_1$ and $L_2$ are 7.5 and 2.5 cm respectively. The detector has a diameter of 2.5 cm. Light

intensity is assumed to be constant within a cone of $4 \times 10^{-2}$ rad and zero outside. The dotted curve represents the case where $L_2$ is removed and the detector is placed at A.

Fig. 5. Time-of-flight experiment on the focal spot. The experimental setup is shown on the left. The U curve on the right was obtained from Eq. (12) using experimentally determined parameters K, $P_o$, and P(t). The dots with the error bars at 21 and 29.5 cm are results obtained from the time-of-flight measurements with respect to the focal spot at the end of the 36-cm cell. The dashed line with a slope equal to the light velocity is shown for comparison.

Fig. 6. Experimental setup with which the input power (P), the backward Raman pulse (BR), backward Brillouin pulse (B), forward Raman pulse (FR), filament pulse (F), and filament picture ($F_p$) can be simultaneously recorded. $D_1$, $D_2$, $D_3$, and $D_4$ are fast detectors.

Fig. 7. A typical set of oscilloscope traces obtained with the setup shown in Fig. 6. for different input laser powers. A toluene cell of 32.5 cm long was used in the experiment. See the text for more detail (Traces on the left, 5 nsec/div.; traces on the right, 2 nsec/div.).

Fig. 8. Oscilloscope traces (5 nsec/div.) of incident ($P_i$) and transmitted ($P_t$) laser pulses through a 26 cm toluene cell.

(a) Below threshold, laser power is not depleted.

(b) Above threshold, laser power is depleted by the backward stimulated scattering.

Fig. 9. (a) Schematic diagram showing the relative positions of the backward Raman pulse initiated at A and the filament pulse. The

pulse separation at $t_2$ (when the focal spot is at the end of the cell) is defined as d.

Fig. 10. Pulse separation d, as a function of input peak power for four different cell lengths. The solid curves are theoretical predictions calculated from the U curves determined by Eq. (12), using experimentally determined values of $P_o$ and K.

Fig. 11. (a) Experimental setup for measuring the spectrum of radiation from a filament using a Fabry-Perot interferometer.

(b) Fabry-Perot patterns of radiation from a filament for the case where self-focusing of a Q-switched pulse yields a focal spot with a velocity several times larger than the light velocity near the end of the cell. The free spectral range of the Fabry-Perot is 1 $cm^{-1}$. The oscilloscope traces (10 nsec/div.) show the corresponding input laser pulses and the sharp backward Raman pulses. It is seen that spectral broadening increases with the input laser power.

Fig. 12. A set of typical laser and Raman Stokes spectra of a filament created by self-focusing of 1.6 nsec mode-locked pulses in a 37 cm toluene cell, taken with the spectrograph focused at the end of the cell; the laser spectra are on the left with the slit images centered at 14402 $cm^{-1}$ and the Stokes spectra on the right with the slit images centered at 13400 $cm^{-1}$.

Fig. 13. (a) Interleafed input laser pulse train and filament pulses. The laser pulses were optically delayed by 6 nsec with respect to the filament pulses. Three filament pulses appeared in this shot.

(b) Interleafed input laser pulse train (optically delayed by 6 nsec) and Raman Stokes pulses from the filaments recorded

simultaneously with (a).

(c) Interleafed input and transmitted laser pulse trains showing depletion of laser energy. The input pulses were optically delayed by 6 nsec with respect to the transmitted pulses. They correspond to the train with lower amplitude.

Fig. 14. (a) Profile and intensity distribution in the local coordinate $\xi = t - zn_o/c$ of a picosecond pulse propagating in space.

(b) Profile and intensity distribution in the local coordinate $\xi = t - zn_o/c$ of a picosecond pulse which has become quasi-stabilized through self-focusing in a Kerr liquid.

Fig. 15. (a) Normalized square amplitude $P_f \equiv A^2$ of the filament output vs time $(A^2_{max}/(2n_2/n_o)k^2a^2 = 4.7 \times 10^3)$.

(b) Field-induced phase change $\Delta\phi$ in the filament $(\Delta\phi_{max} = 225$ rad.)

(c) Power spectrum of the filament output obtained from Fourier transform of $A \exp(i\Delta\phi)$.

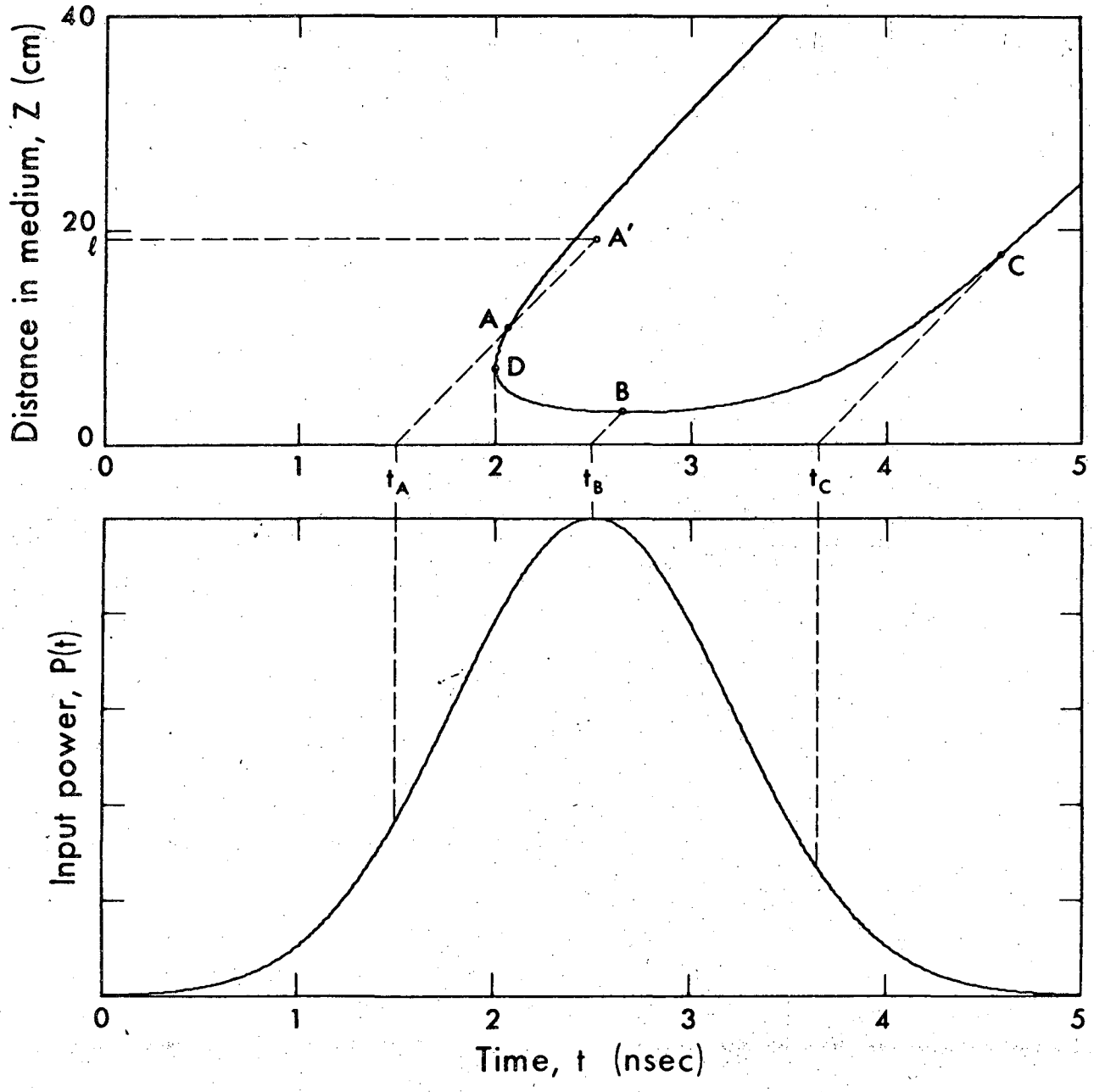


XBL 7010-6738

Fig. 1

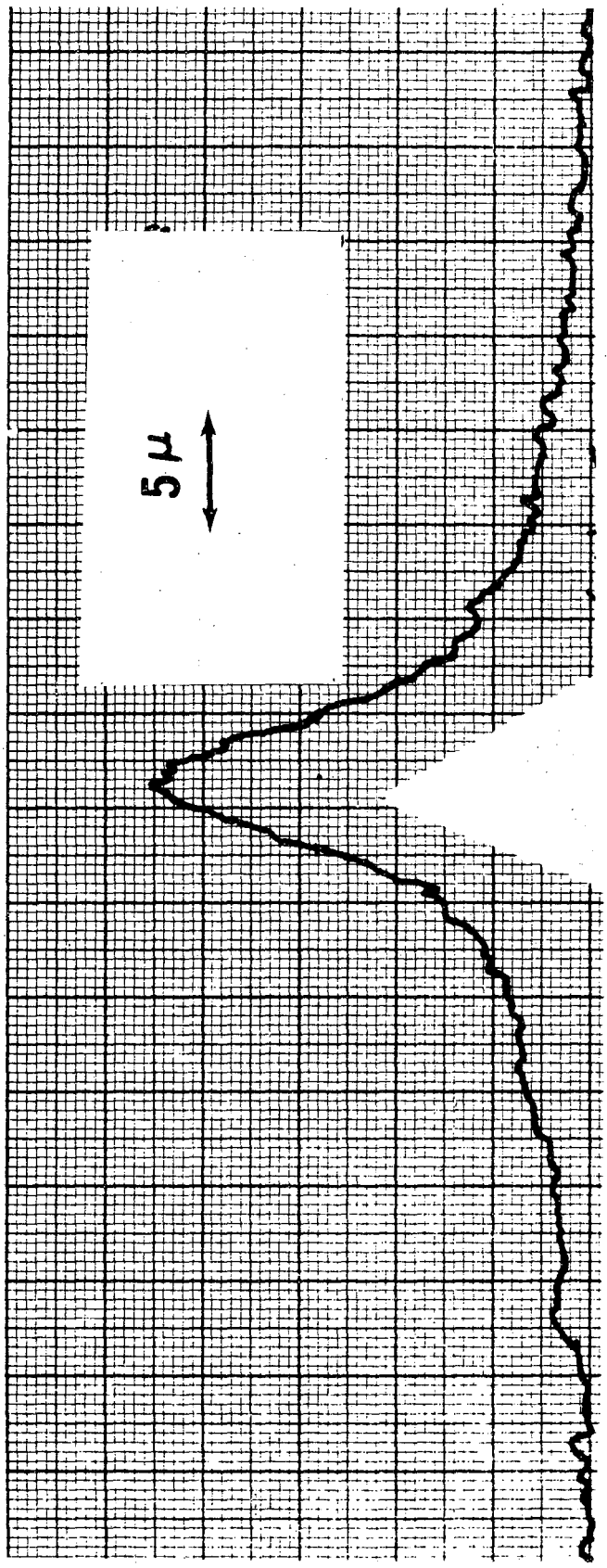


XBL715-6739

Fig. 2

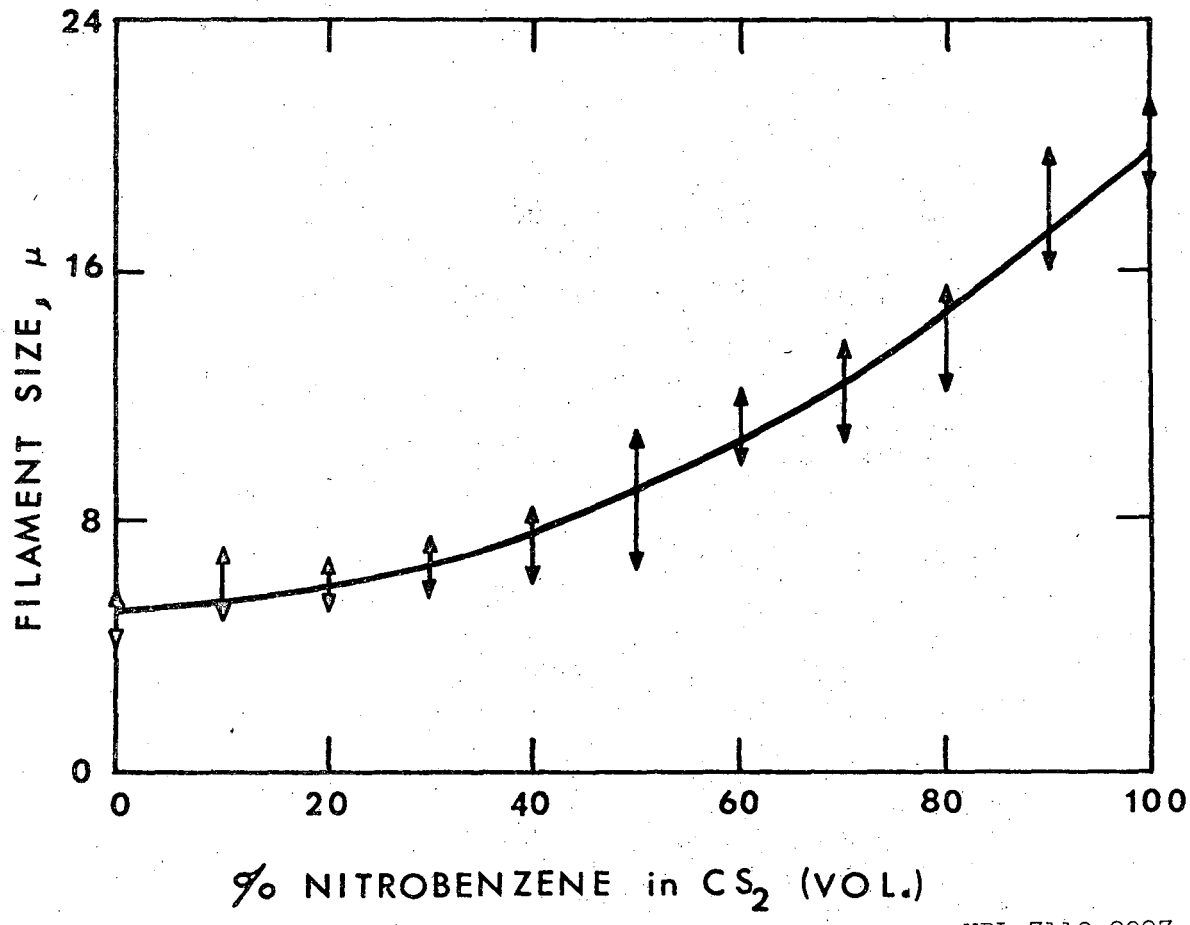


XBL-7112-2297

Fig. 3

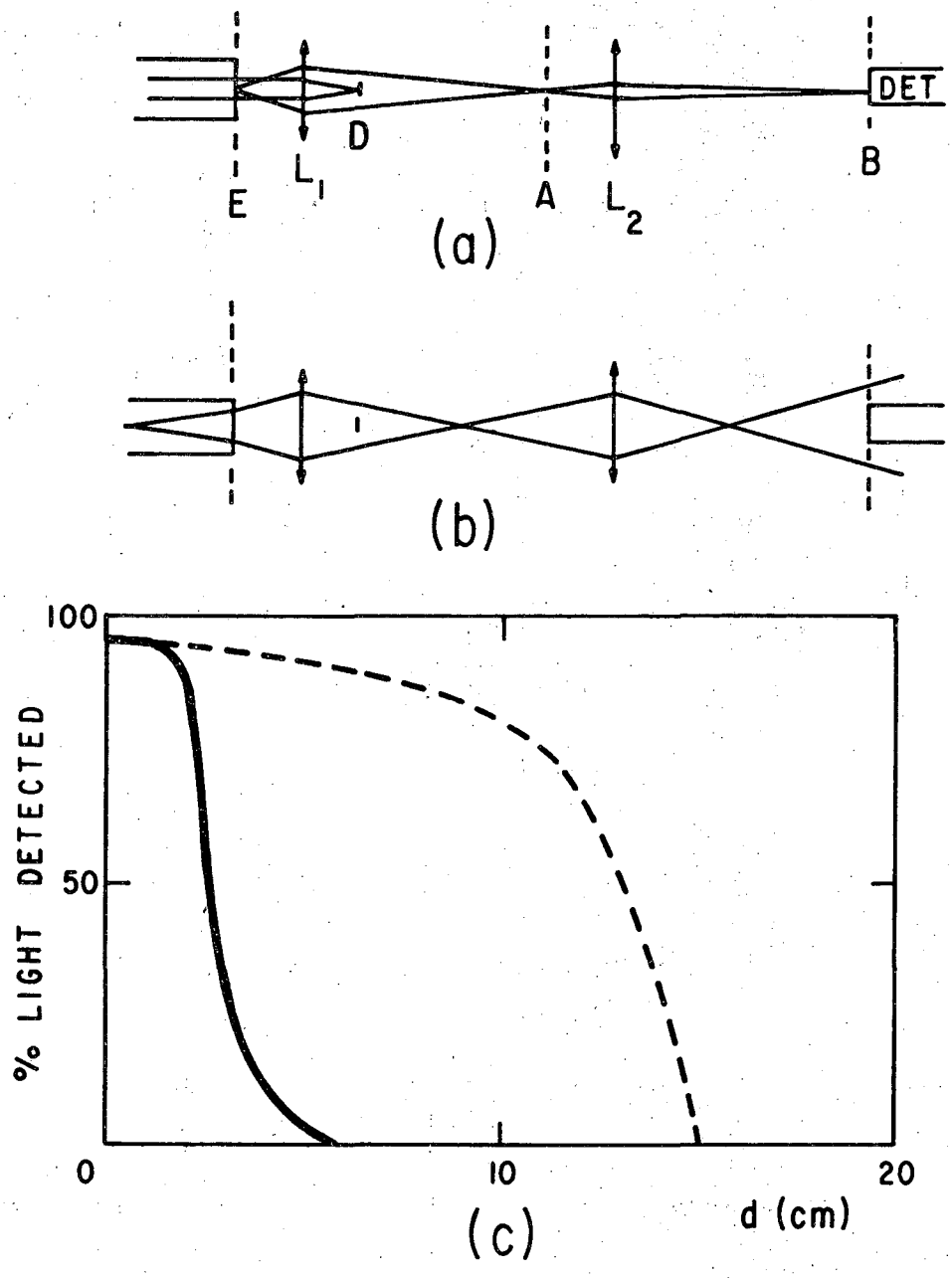


XBL-7112-2296

Fig. 4

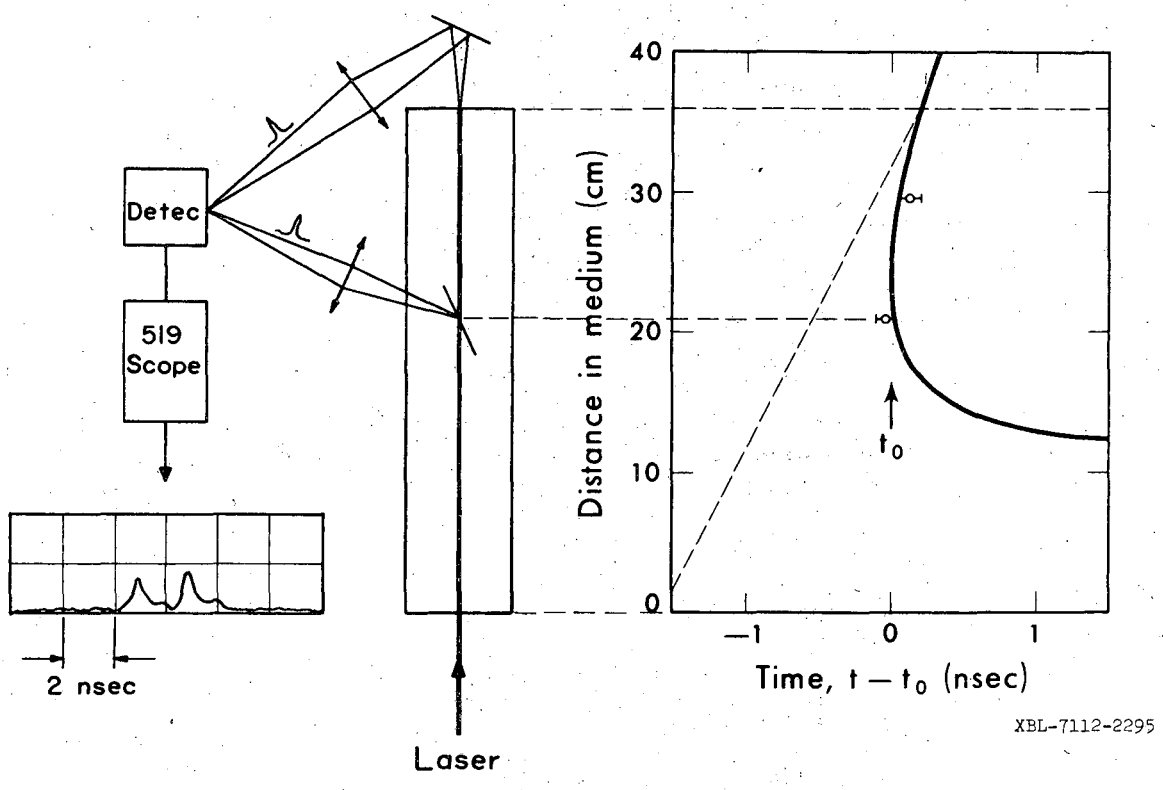
Detec
519
Scope
2 nsec
Laser
Distance in medium (cm)
40
30
20
10
0
−1
0
1
Time, t − t0 (nsec)
t0
XBL-7112-2295

Fig. 5

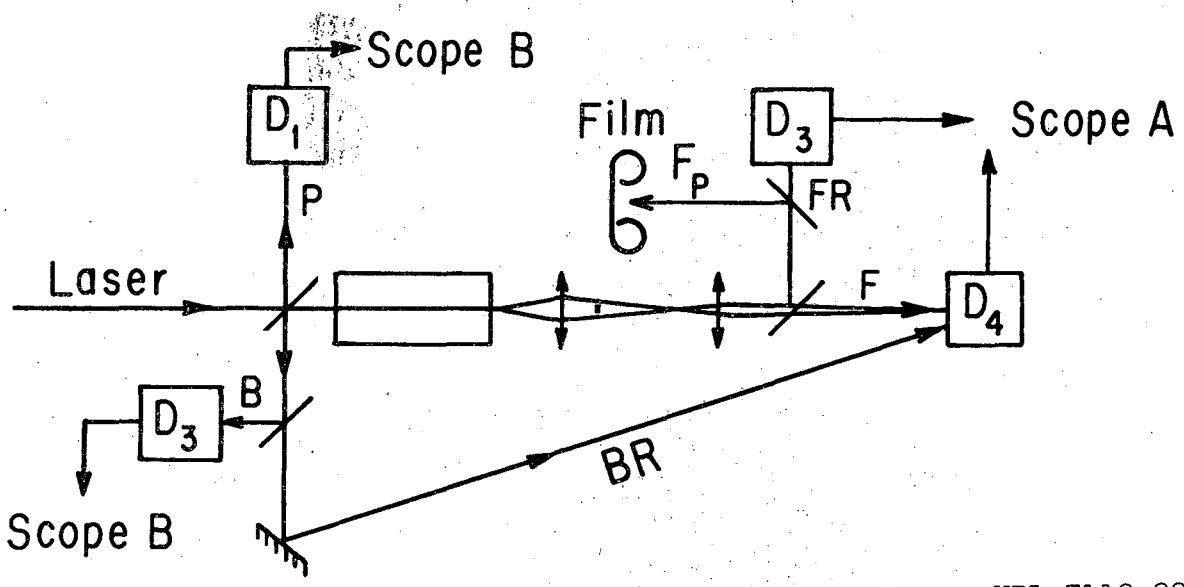


XBL-7112-2292

Fig. 6

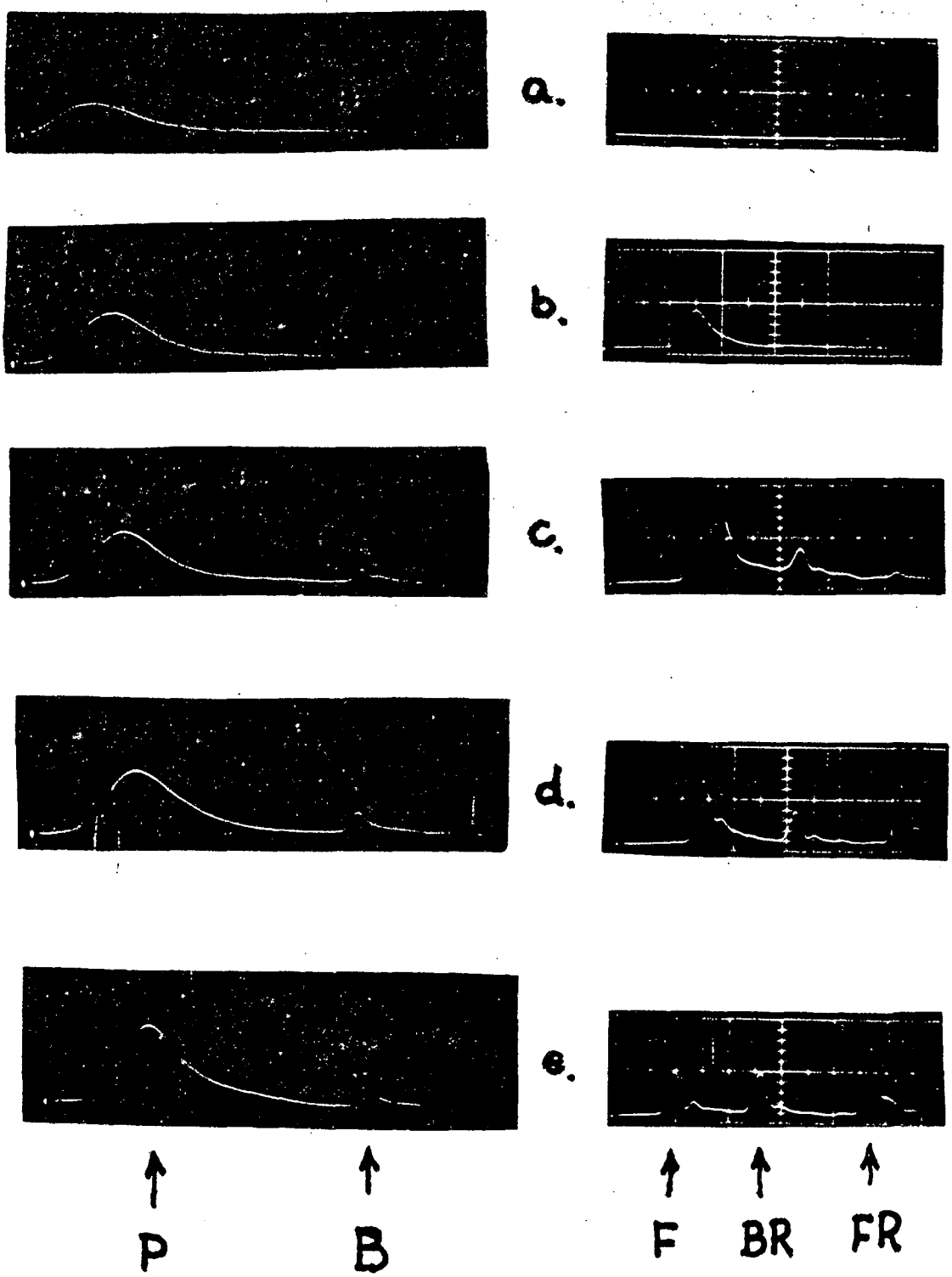


Fig. 7

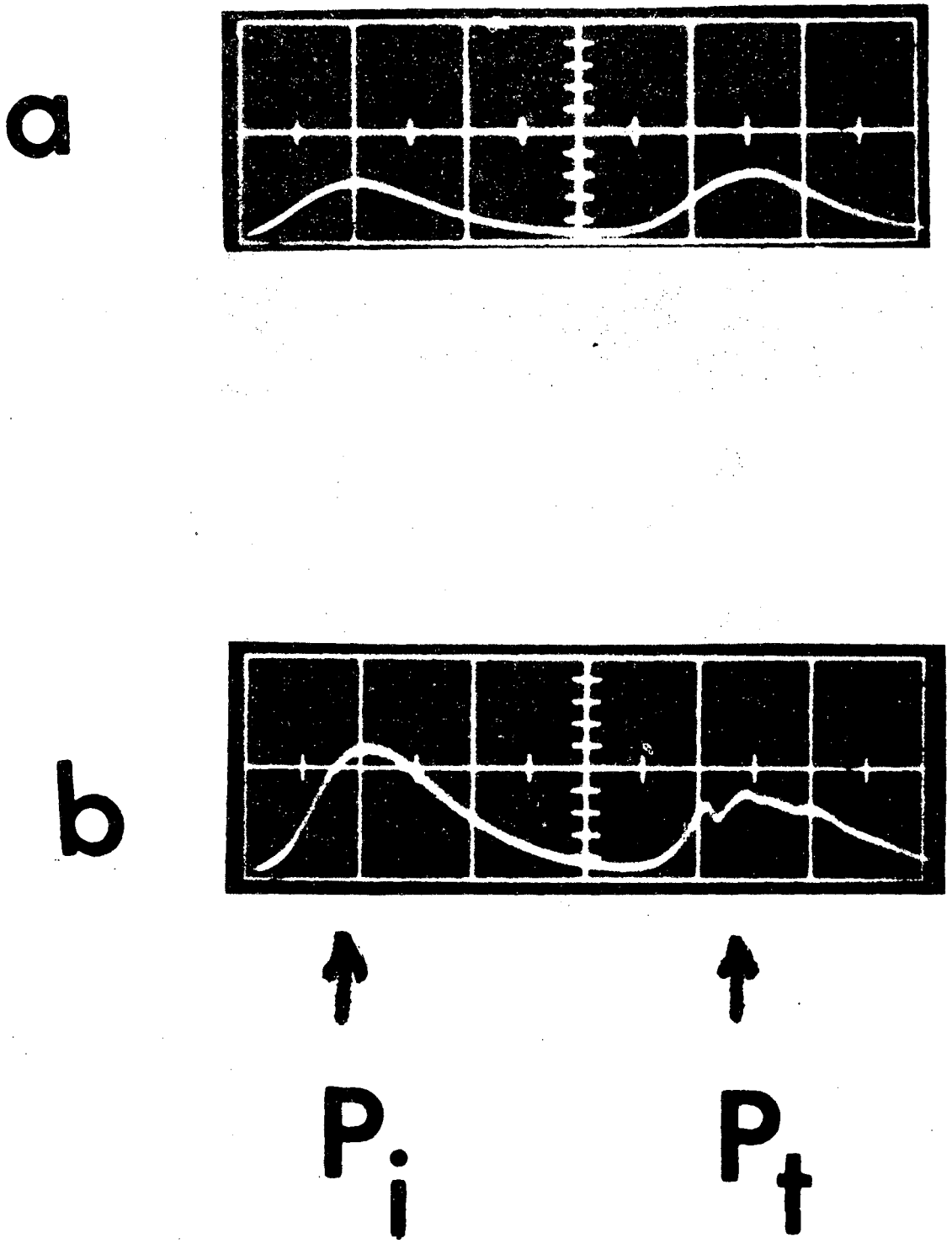


Fig. 8

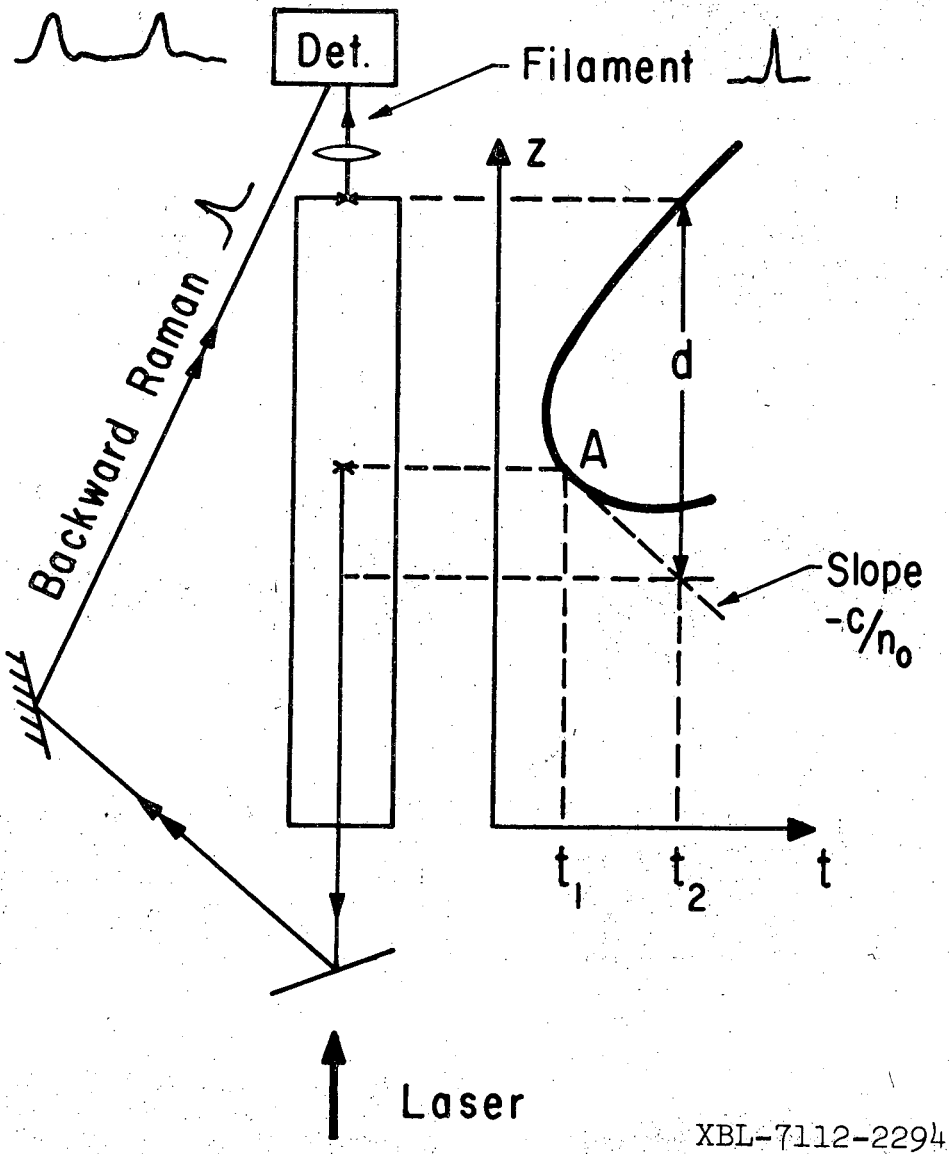


XBL-7112-2294

Fig. 9

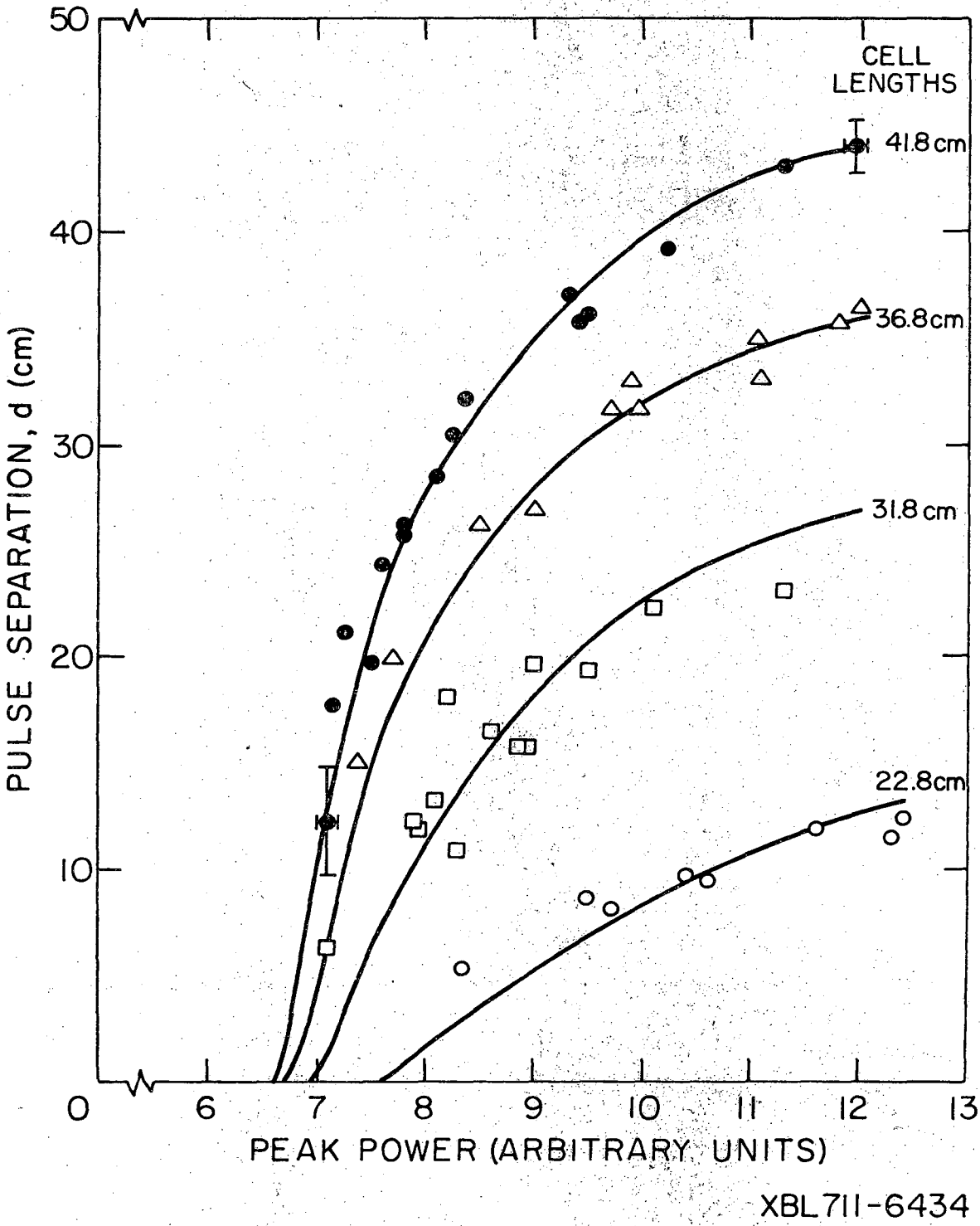
CELL LENGTHS
41.8 cm
36.8 cm
31.8 cm
22.8 cm
PULSE SEPARATION, d (cm)
PEAK POWER (ARBITRARY UNITS)
0
10
20
30
40
50
6
7
8
9
10
11
12
13
XBL711-6434

Fig. 10

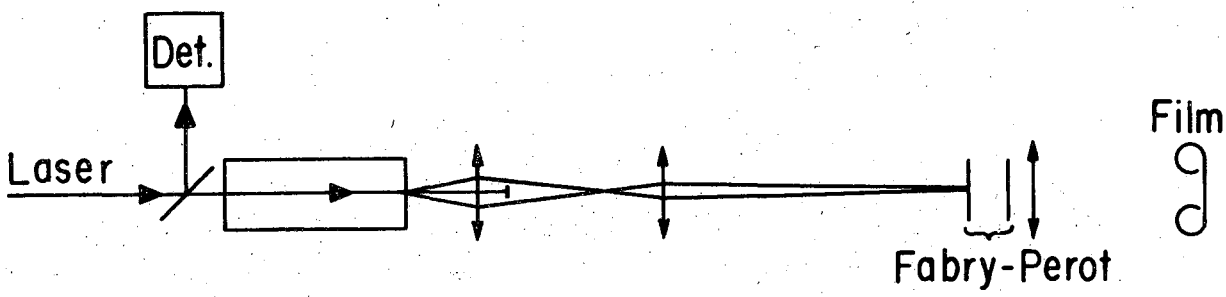


XBL-7112-2293

Fig. 11(a)

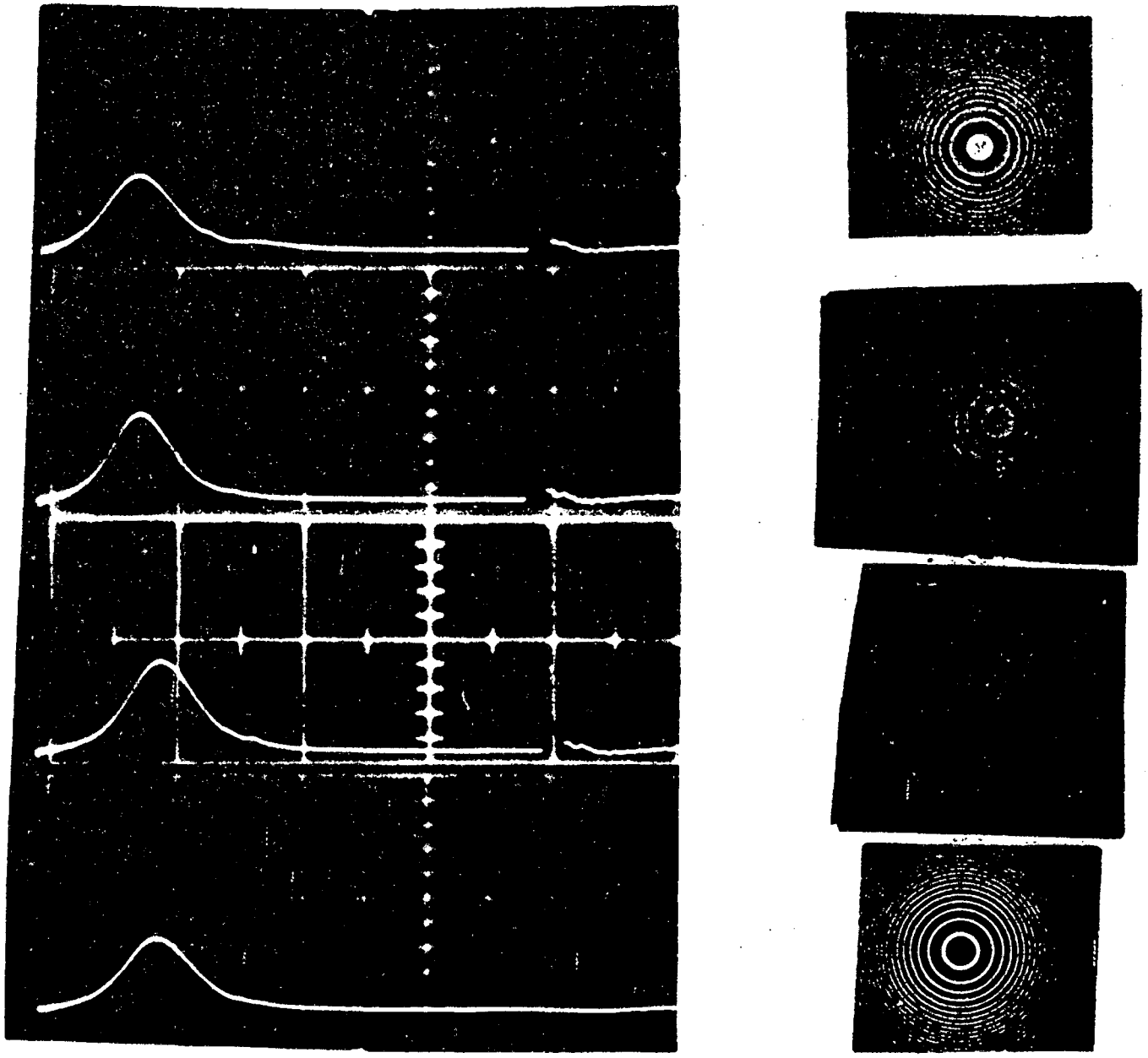

Fig. 11(b)

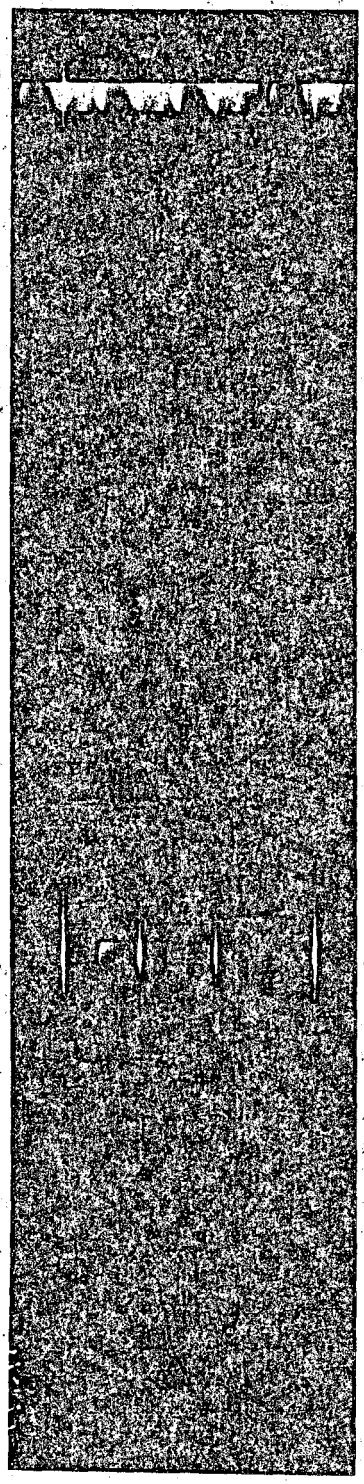

Fig. 12

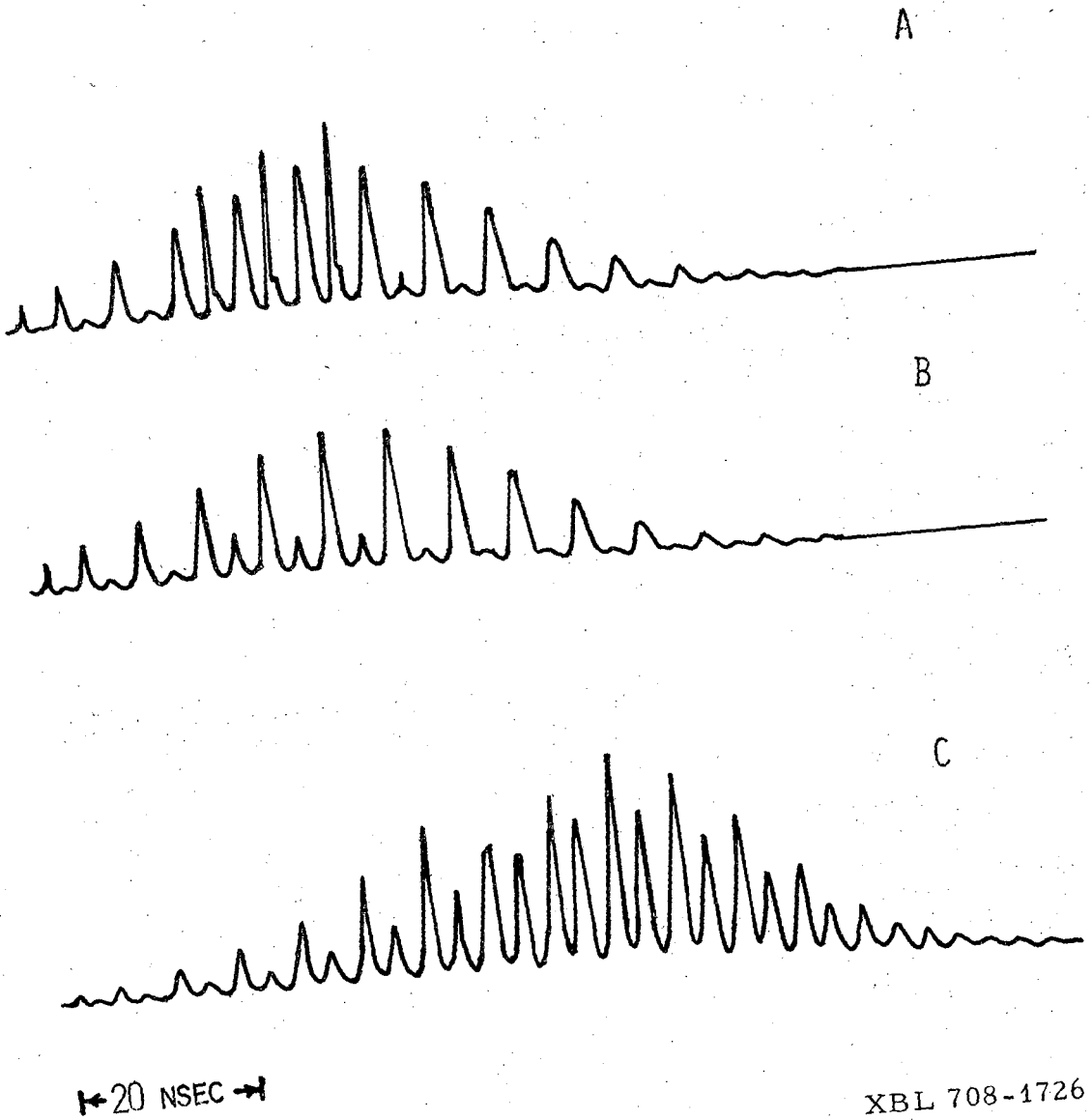


Fig. 13

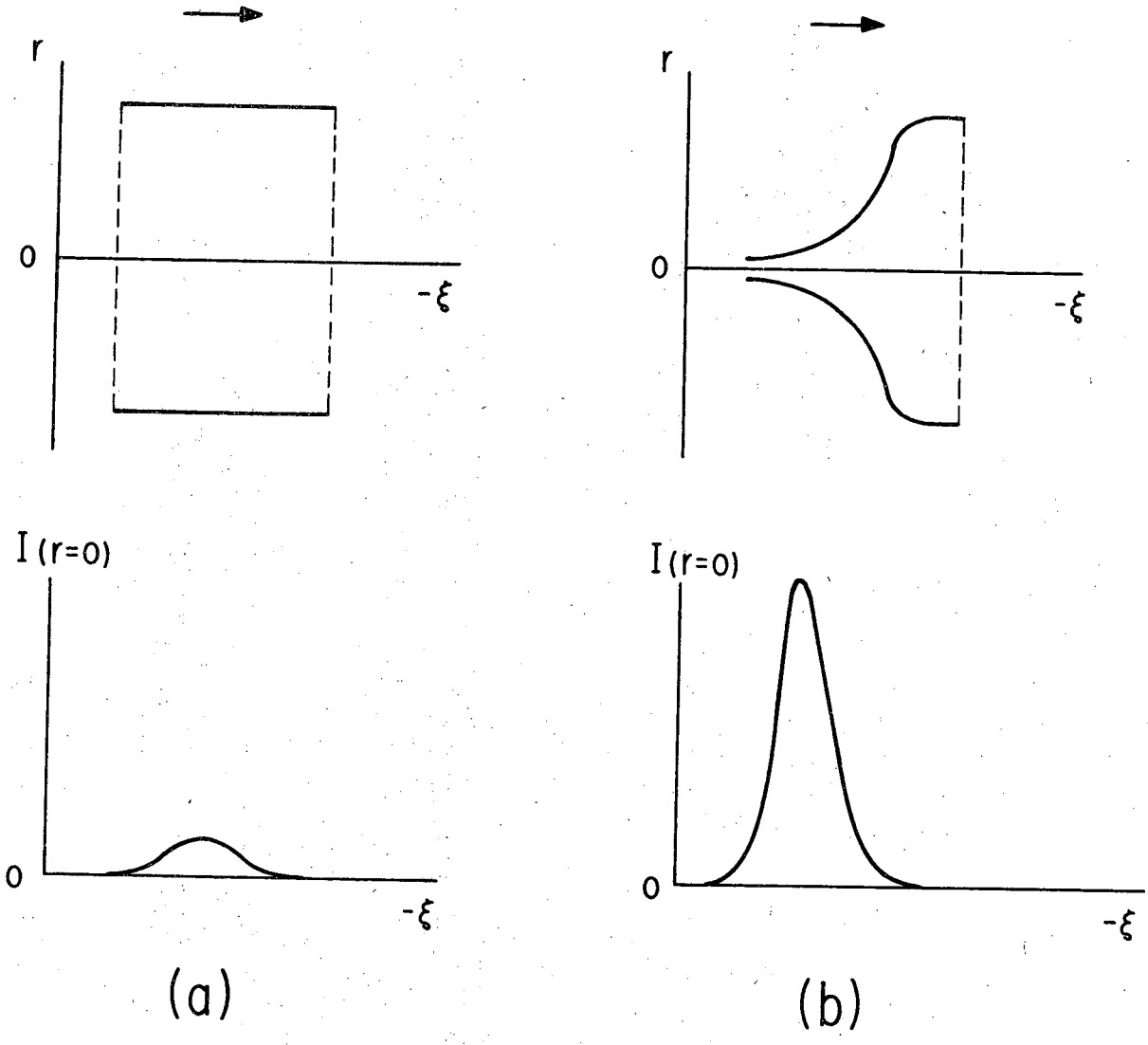


XBL-7112-2291

Fig. 14

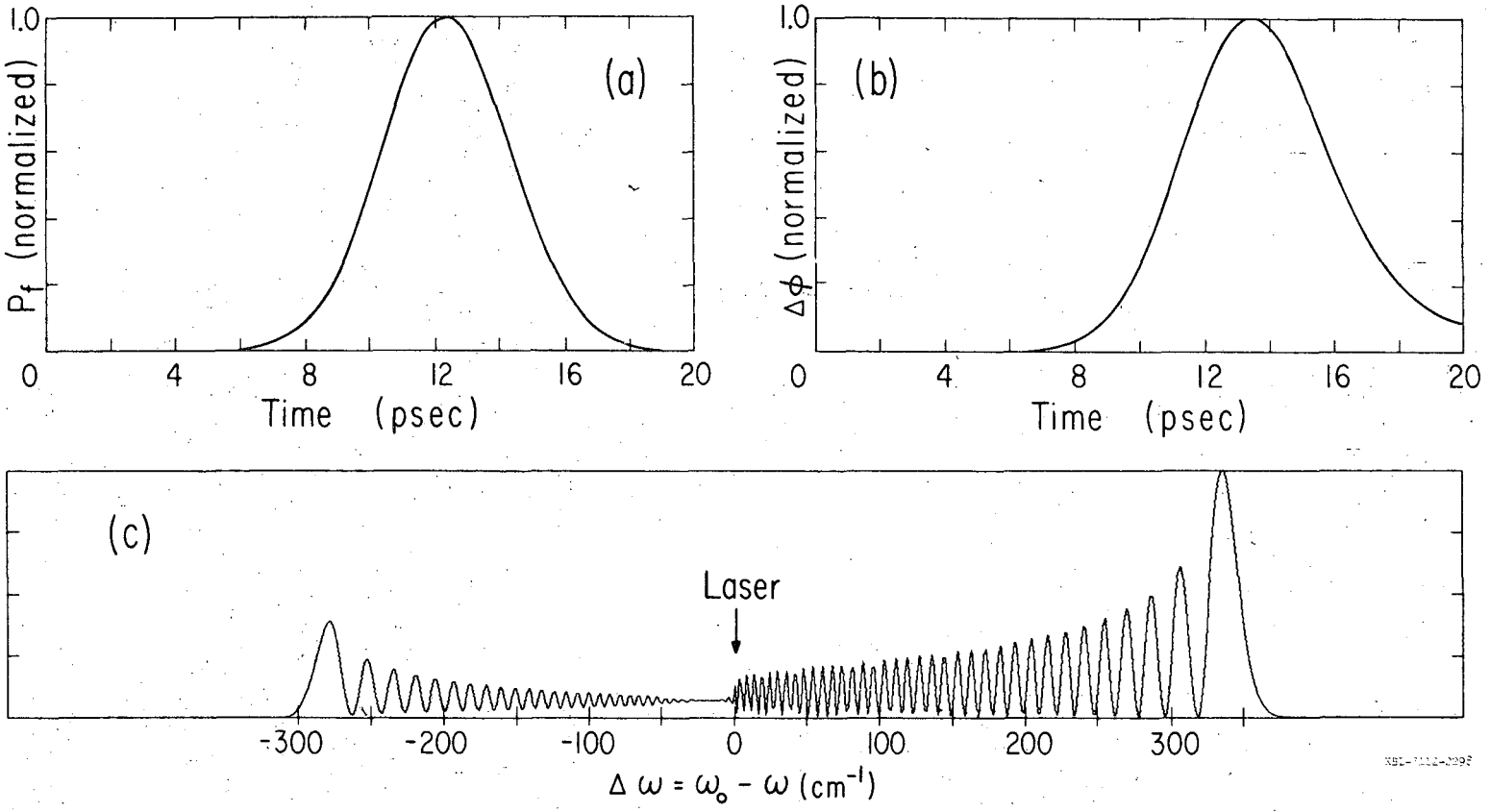
1.0
$P_f$ (normalized)
(a)
0
4
8
12
16
20
Time (psec)
1.0
$\Delta\phi$ (normalized)
(b)
0
4
8
12
16
20
Time (psec)
(c)
Laser
-300
-200
-100
0
100
200
300
$\Delta\omega = \omega_o - \omega$ (cm$^{-1}$)

Fig. 15

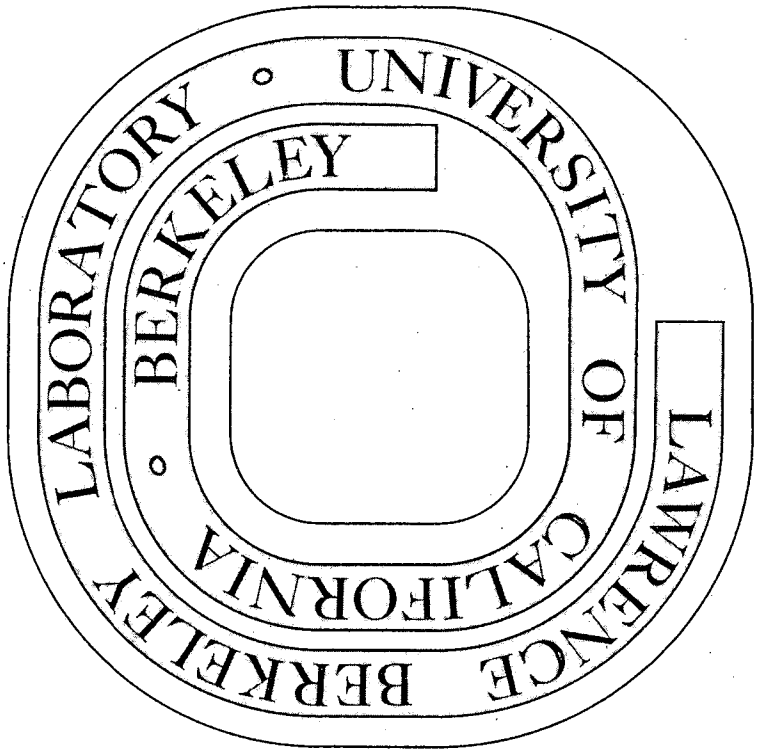
LAWRENCE BERKELEY LABORATORY
UNIVERSITY OF CALIFORNIA
BERKELEY